

Theoretical Study of the Hydration of Atmospheric Nucleation Precursors with Acetic Acid

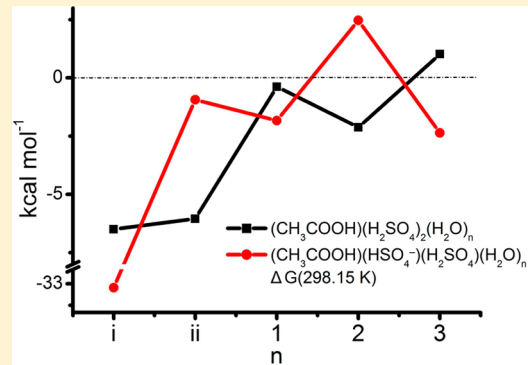
Yu-Peng Zhu,[†] Yi-Rong Liu,[†] Teng Huang,[†] Shuai Jiang,[†] Kang-Ming Xu,[†] Hui Wen,[†] Wei-Jun Zhang,^{†,‡} and Wei Huang^{*,†,‡}

[†]Laboratory of Atmospheric Physico-Chemistry, Anhui Institute of Optics & Fine Mechanics, Chinese Academy of Sciences, Hefei, Anhui 230031, China

[‡]School of Environmental Science & Optoelectronic Technology, University of Science and Technology of China, Hefei, Anhui 230026, China

Supporting Information

ABSTRACT: While atmosphere is known to contain a significant fraction of organic substance and the effect of acetic acid to stabilize hydrated sulfuric acids is found to be close that of ammonia, the details about the hydration of $(\text{CH}_3\text{COOH})(\text{H}_2\text{SO}_4)_2$ are poorly understood, especially for the larger clusters with more water molecules. We have investigated structural characteristics and thermodynamics of the hydrates using density functional theory (DFT) at PW91PW91/6-311++G(3df,3pd) level. The phenomena of the structural evolution may exist during the early stage of the clusters formation, and we tentatively proposed a calculation path for the Gibbs free energies of the clusters formation via the structural evolution. The results in this study supply a picture of the first deprotonation of sulfuric acids for a system consisting of two sulfuric acid molecules, an acetic acid molecule, and up to three waters at 0 and 298.15 K, respectively. We also replace one of the sulfuric acids with a bisulfate anion in $(\text{CH}_3\text{COOH})(\text{H}_2\text{SO}_4)_2$ to explore the difference of acid dissociation between two series of clusters and interaction of performance in clusters growth between ion-mediated nucleation and organics-enhanced nucleation.



1. INTRODUCTION

Atmospheric aerosols play a critical role in the earth-atmosphere system, including influencing the Earth radiation budget, cloud formation, human health, photochemical chemistry, and partitioning of trace species by providing surfaces for heterogeneous chemical reactions.^{1–5} As an integral part of atmosphere, aerosols can be directly released into the atmosphere from natural and anthropogenic sources or formed in the atmosphere via nucleation from gas-phase species. New particle formation produces a large proportion of atmospheric aerosols and has been commonly observed in various environments, including urban, forested and remote continental areas.⁶ The formation of new particles proceeds through two phases, i.e., a nucleation phase leading to a metastable critical cluster ($\sim 1\text{--}3$ nm in diameter) and a growth phase where the critical cluster increases readily in size.^{7,8} An accurate physical understanding of nucleation is essential and it seems to be difficult due to the challenge of detecting, counting, and determining the exact composition of these molecular clusters as they grow to a critical cluster in experiments.^{9–15}

Several mechanisms have been proposed to explain nucleation events in the continental troposphere, including binary $\text{H}_2\text{SO}_4/\text{H}_2\text{O}$ and ternary $\text{H}_2\text{SO}_4/\text{H}_2\text{O}/\text{NH}_3$ nucleation, ion-mediated nucleation, and nucleation enhanced by organic compounds.⁸ Sulfuric acid has been widely identified as one of

the major atmospheric nucleating species.^{9,16} The importance of organic species in aerosol nucleation has been recently realized.^{17–21} Organic compounds from anthropogenic and biogenic emissions react with atmospheric oxidants to form a number of products,^{22–24} including organic carbonyls and acids, some of which may participate in nucleation and growth to form nanoparticles under various environments.^{25,26} The presence of organic acids considerably enhances new particle formation of the water-sulfuric acid system via formation of strongly hydration-bonded clusters containing one molecule of an organic acid and several molecules of sulfuric acid and water.^{9,19,21,27} Compared to homogeneous nucleation involving neutral clusters, the nucleation on ions is favored due to the small charged clusters with much more thermodynamic stability.²⁸ Besides, ionic clusters grow faster than neutrals due to the dipole–charge interaction between charged clusters and strongly dipolar precursor molecules.²⁹ Our insight into nucleation is incomplete because the nucleation mechanism can be different due to the changes in many aspects such as region, time, elevation, and anthropokinetics.

Received: June 23, 2014

Revised: August 19, 2014

Published: August 21, 2014

Hydration of acids plays a key role in the atmosphere³⁰ as a source of aerosol nucleation intermediates and catalytic agents in many reactions. Therefore, a clear and insightful understanding of these phenomena is essential for modeling atmospheric processes.³¹ The most trustworthy computational studies of sulfuric acid hydrate formation by now are provided from the Helsinki group,³² and the results are close to the available experimental values of Hanson and Eisele,³³ and also the Shields group.^{7,34} In terms of common organic acids, the interaction of five dicarboxylic acids with sulfuric acid and ammonia has been studied by the Zhang group, employing quantum chemical calculations, quantum theory of atoms in molecules (QTAIM), and the natural bond orbital (NBO) analysis methods.⁶ In addition, the interaction of the common organic oxalic acid with atmospheric nucleation precursors and trace ion species has been investigated by the Yu group using density functional theory (DFT).³⁵ Although dicarboxylic acids enhance nucleation in two directions,⁶ in contrast to monocarboxylic acid, we put the insight into acetic acid due to its wide range of natural and anthropogenic sources and closely correlation with human life. The stabilizing effect of acetic acid is also found to be close that of ammonia,²⁰ and the details about the hydration of $(\text{CH}_3\text{COOH})(\text{H}_2\text{SO}_4)_2$ are poorly understood, especially for the larger clusters with more water molecules. In the present study, the hydration of $(\text{CH}_3\text{COOH})(\text{H}_2\text{SO}_4)_2$ is studied using DFT at PW91PW91/6-311++G(3df,3pd) level. We searched for the minimum energy structures of $(\text{CH}_3\text{COOH})(\text{H}_2\text{SO}_4)_2(\text{H}_2\text{O})_{n=i,ii,1-3}$ and determined the thermodynamic properties of these clusters. Here, $n = i$ corresponds to sulfuric acid dimer, $(\text{H}_2\text{SO}_4)_2$, and $n = ii$ stands for acid trimer, $(\text{CH}_3\text{COOH})(\text{H}_2\text{SO}_4)_2$. A further insight into the nature of sulfuric acid dissociation at a molecular level can be gained in this study. According to the trend of structural evolution during the early stage of clusters formation, we tentatively proposed a calculation path for the Gibbs free energies of clusters formation at 298.15 K. Moreover, we replace one of the sulfuric acids with a bisulfate anion in $(\text{CH}_3\text{COOH})(\text{H}_2\text{SO}_4)_2$ to explore the differences of acid dissociation between two series of clusters and interaction of performance in clusters growth between ion-mediated nucleation and organics-enhanced nucleation. For the $(\text{CH}_3\text{COOH})(\text{HSO}_4^-)(\text{H}_2\text{SO}_4)(\text{H}_2\text{O})_{n=i,ii,1-3}$ clusters, $n = i$ equals to $(\text{HSO}_4^-)(\text{H}_2\text{SO}_4)$, and $n = ii$ amounts to $(\text{CH}_3\text{COOH})(\text{HSO}_4^-)(\text{H}_2\text{SO}_4)$. This work is a continuation of long-standing efforts to explore ion–molecule interactions,^{36–44} hydrogen-bonded interactions,^{45–57} water cluster formation,^{42,45,48,56,58–66} and atmospheric process.^{34,41,43,44,67–72}

2. METHODS

The initial/generated geometries were obtained with Basin-Hopping (BH) algorithm, and PW91/DND implemented in DMol3 was employed in the DFT module coupled with BH, where PW91 means the gradient-corrected correlation functional proposed by Perdew and Wang, in 1991, and DND refers to double numerical plus d-functions basis set. Then the results were optimized at PW91PW91/6-31+G* level by DFT. The stable isomers within 10 kcal mol⁻¹ of the stable global minimum obtained from the first optimization have been optimized using the PW91PW91/6-311++G(3df,3pd) method to get the final configurations. It will take much less time to get the final structures with twice optimizations, rather than only once direct optimization via the PW91PW91/6-311++G(3df,3pd) method. For each stationary point, frequency calculations have been operated to ensure there were no imaginary frequencies.

The convergence standards used for the optimization are default setting in Gaussian09 software. Finally, the optimized geometries have been taken in single point energy calculations using DF-MP2-F12 (second-order Møller–Plesset perturbation theory-explicitly correlated methods with density fitting). Zero-point corrected energies [$E(0)$], energies including atmospheric temperature enthalpies [$H(T)$] and Gibbs free energies [$G(T)$], can be evaluated by combining the PW91PW91/6-311++G(3df,3pd) thermodynamic corrections with DF-MP2-F12 single point energies.

Apart from the traditional calculation for Gibbs free energies of clusters formation, obtained by subtraction between the Gibbs free energies of global minima of products and reactants, we proposed a tentative calculation path: the fit local (maybe global) minimum among the reactant isomers can be found according to the trend of structural evolution⁷³ while the global minimum of product can be confirmed by the order of the increasing Gibbs free energies, then, the Gibbs free energy of cluster formation can be obtained by subtraction between Gibbs free energy of global minimum of product and Gibbs free energies of the fit local (maybe global) minimum of the reactants. To investigate the error limit of the tentative calculation path, we also calculated the Boltzmann averaged binding energies⁷ at the PW91PW91/6-311++G(3df,3pd) level of theory for describing the average conditions in the formation of the $(\text{CH}_3\text{COOH})(\text{H}_2\text{SO}_4)_2(\text{H}_2\text{O})_n$ clusters (Details can be seen in the Supporting Information). Furthermore, we calculated the enthalpies of clusters formation via the single point electronic energies from DF-MP2-F12 and the thermal corrections from PW91PW91/6-311++G(3df,3pd).

The choice of the theoretical method is based on the fine performance of PW91PW91 on large amount of atmospheric clusters, especially for aerosol particles containing the common organic acids, including predictions of structural characteristics, the Gibbs free energies and satisfactory similarity compared with experimental data.^{6,35,74,75}

3. RESULTS

The optimized geometry of acetic acid (AA) at PW91PW91/6-311++G(3df,3pd) level of theory are presents in Figure 1.

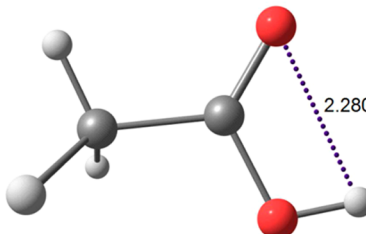


Figure 1. Optimized geometry of acetic acid (AA) at the PW91PW91/6-311++G(3df, 3pd) level (red for oxygen, white for hydrogen, gray for carbon).

The 38 minima located in this study for $(\text{CH}_3\text{COOH})(\text{H}_2\text{SO}_4)_2(\text{H}_2\text{O})_{n=i,ii,1-3}$ are shown in Figure 2–6 while the 34 minima located in the study for $(\text{CH}_3\text{COOH})(\text{HSO}_4^-)(\text{H}_2\text{SO}_4)(\text{H}_2\text{O})_{n=i,ii,1-3}$ are displayed in Figure 7–11, both in order of increasing electronic energy. Among the clusters of $(\text{CH}_3\text{COOH})(\text{H}_2\text{SO}_4)_2(\text{H}_2\text{O})_{n=i,ii,1-3}$, the structures are labeled “I” if the cluster remains intact as $(\text{CH}_3\text{COOH})(\text{H}_2\text{SO}_4)_2(\text{H}_2\text{O})_n$, “II” if one sulfuric acid undergoes a first acid dissociation to form $(\text{CH}_3\text{COOH})(\text{H}_2\text{SO}_4)(\text{HSO}_4^- \text{H}_3\text{O}^+)(\text{H}_2\text{O})_{n-1}$,

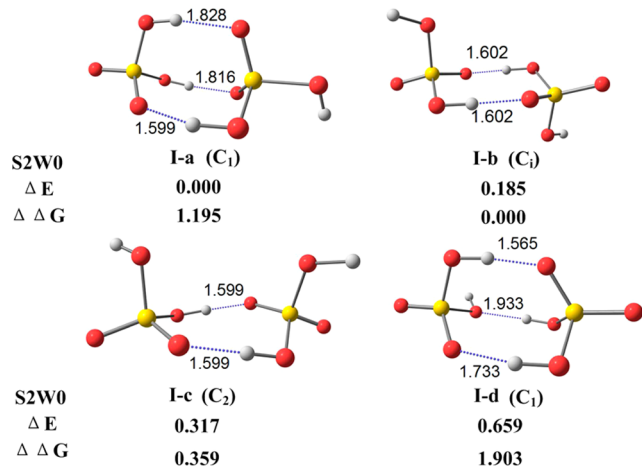


Figure 2. Optimized geometries of $(\text{H}_2\text{SO}_4)_2$ (S2W0) at the PW91PW91/6-311++G(3df, 3pd) level, ordered by increasing ΔE . ΔE represents the relative electronic energy to the global minimum at a standard state of 0 K and 1 atm, and $\Delta \Delta G$ represents the relative free energy of cluster formation to the global minimum at a standard state of 298.15 K and 1 atm (red for oxygen, white for hydrogen, gray for carbon, and yellow for sulfur).

and “III” if both sulfuric acids undergo a first acid dissociation to form $(\text{CH}_3\text{COOH})(\text{HSO}_4^-)(\text{H}_3\text{O}^+)_2(\text{H}_2\text{O})_{n-2}$. In term of the clusters of $(\text{CH}_3\text{COOH})(\text{HSO}_4^-)(\text{H}_2\text{SO}_4)(\text{H}_2\text{O})_{n=i,i,1-3}$, the structures are labeled “I” if the cluster remains intact as $(\text{CH}_3\text{COOH})(\text{HSO}_4^-)(\text{H}_2\text{SO}_4)(\text{H}_2\text{O})_n$, and “II” if the sulfuric acid undergoes a first acid dissociation to form $(\text{CH}_3\text{COOH})(\text{HSO}_4^-)_2(\text{H}_2\text{O}^+)(\text{H}_2\text{O})_{n-1}$.

The binding electronic energies, enthalpies, and free energies for the clusters $(\text{CH}_3\text{COOH})(\text{H}_2\text{SO}_4)_2(\text{H}_2\text{O})_{n=i,i,1-3}$ at 0 and 298.15 K obtained at the PW91PW91/6-311++G(3df,3pd) level of theory are displayed in Tables 1–4. Similarly, The binding electronic energies, enthalpies, and free energies for the clusters $(\text{CH}_3\text{COOH})(\text{HSO}_4^-)(\text{H}_2\text{SO}_4)(\text{H}_2\text{O})_{n=i,i,1-3}$ at

0 and 298.15 K obtained at the PW91PW91/6-311++G(3df,3pd) level of theory are shown in Tables 5–8. Tentative calculations for the Gibbs free energies of clusters formation via the structural evolution can be seen in Table 1–8 (Details can be seen in the Supporting Information). Table 9 contains the Boltzmann averaged binding energies at the PW91PW91/6-311++G(3df,3pd) level of theory for the formation of the $(\text{CH}_3\text{COOH})(\text{H}_2\text{SO}_4)_2(\text{H}_2\text{O})_n$ and $(\text{CH}_3\text{COOH})(\text{HSO}_4^-)(\text{H}_2\text{SO}_4)(\text{H}_2\text{O})_n$ clusters displayed in the figures.

The dissociation of sulfuric acid with water into ion pairs can occur in small gas-phase clusters such as the dimer hydrates invested in Temelso and Shields’ study.⁷ We explored the details of the dissociation in trimer hydrates in this study. As Figure 12 shows, the first acid dissociation of one of the sulfuric acids occurs in the presence of first water at 0 K and two waters at 298.15 K. Both sulfuric acids of the trimer hydrate undergo first acid dissociation to two bisulfate anions and two hydronium cations in the presence of three waters at 0 K, and it seems to be dramatically difficult at room temperature. Replacing one of sulfuric acids with a bisulfate anion delays the start of dissociation and puts it off to two waters at 0 K and three waters at 298.15 K as described in Figure 13. The comparison between three types of calculation for the free energies of clusters formation in the growth of the $(\text{CH}_3\text{COOH})(\text{H}_2\text{SO}_4)_2(\text{H}_2\text{O})_n$ clusters at room temperature are shown in Figure 14 and this process becomes thermodynamically favorable with fluctuations. Similar comparison for the $(\text{CH}_3\text{COOH})(\text{HSO}_4^-)(\text{H}_2\text{SO}_4)(\text{H}_2\text{O})_n$ clusters are displayed in Figure 15. The replacement with a bisulfate anion impairs the thermodynamic fluctuations and changes the favorable steps in the clusters growth. The thermodynamics for the growth of two series of clusters up to three waters are displayed in Figure 16.

4. DISCUSSION

4.1. Structures. Acetic acid has a dipole moment of 1.74 D, and the dipole moment of sulfuric acid is 2.96 D while the complex with waters has dipole moments ranging from 2.6 to 3.0 D.

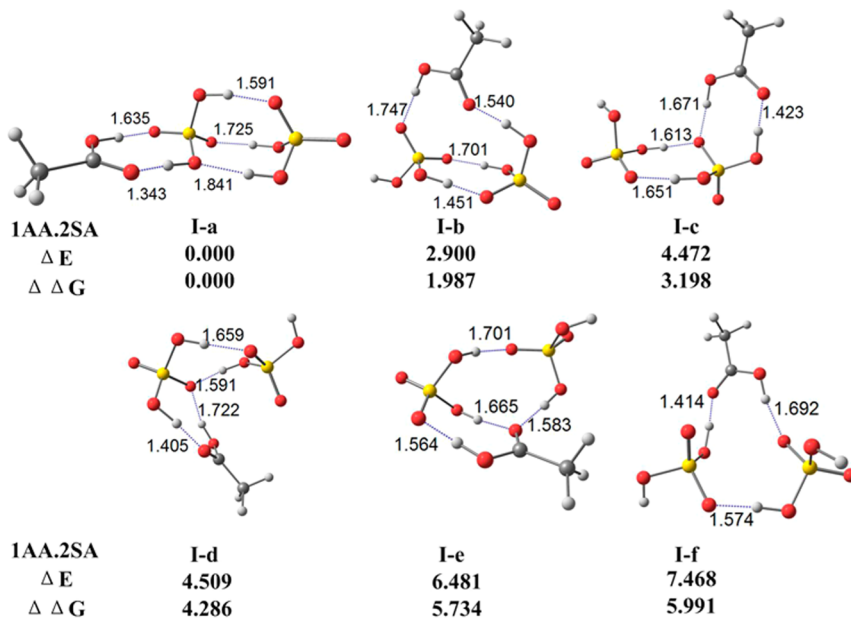


Figure 3. Optimized geometries of $(\text{CH}_3\text{COOH})(\text{H}_2\text{SO}_4)_2$ (1AA.2SA) at the PW91PW91/6-311++G(3df,3pd) level, ordered by increasing ΔE . ΔE represents the relative electronic energy to the global minimum at a standard state of 0 K and 1 atm, and $\Delta \Delta G$ represents the relative free energy of cluster formation to the global minimum at a standard state of 298.15 K and 1 atm.

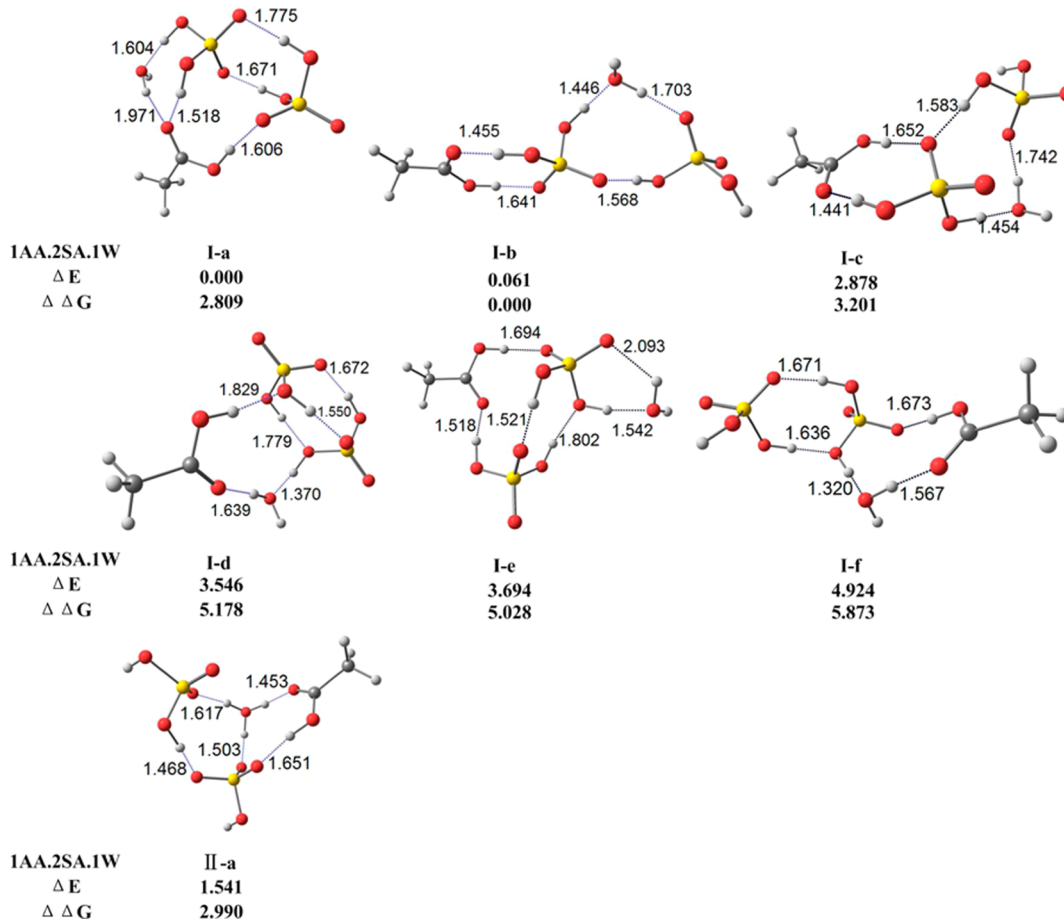


Figure 4. Optimized geometries of $(\text{CH}_3\text{COOH})(\text{H}_2\text{SO}_4)_2(\text{H}_2\text{O})$ (IAA.2SA.1W) at the PW91PW91/6-311++G(3df,3pd) level, ordered by state of dissociation (I, II, III) and increasing ΔE . ΔE represents the relative electronic energy to the global minimum at a standard state of 0 K and 1 atm, and $\Delta \Delta G$ represents the relative free energy of cluster formation to the global minimum at a standard state of 298.15 K and 1 atm.

It has extremely strong interactions between acetic acid, sulfuric acid and waters, lead to the search for all possible configurations of these complexes challenging.⁷ We have widely and repetitiously sampled the local minima in order to locate a convincing set of various structures for each set of clusters.

Figure 1 shows that the acetic acid monomer, CH_3COOH , has a carboxyl group and a methyl group. In solid acetic acid, the molecules form pairs (dimers), being connected by hydrogen bonds. The dimer can be detected in the vapor at 393 K, and it also can be found in the liquid phase in dilute solutions in non-hydrogen-bonding solvents, and a certain extent in pure acetic acid, but are disrupted by hydrogen-bonding solvents.⁷⁶

As shown in Figure 2, the sulfuric acid dimers, $(\text{H}_2\text{SO}_4)_2$, have four isomers in close electronic energetic propinquity (within 0.7 kcal mol⁻¹). The I-a and I-d isomers, are composed of one *cis*- and one *trans*- H_2SO_4 and have C_1 symmetry. The I-b and I-c isomers are composed of two *trans*- H_2SO_4 monomers with C_i and C_2 symmetry, respectively. The I-a (C_1) isomer has three strong hydrogen bonds, making it the electronic energy minimum. The I-d (C_1) isomer also has three hydrogen bonds, but one is a weaker $\text{OH}\cdots\text{OH}$ interaction, as opposed to the stronger $\text{OH}\cdots\text{O}$ bonds found in I-a (C_1). The I-b (C_i) dimer, arranged in a trans-trans configuration, merely has two strong hydrogen bonds and its higher rotational entropy makes it the free energy minimum of cluster formation. The I-c (C_2) dimer has two strong hydrogen bonds, but it is less stable than I-b (C_i) due to the propinquity of the two free hydroxyl groups

and its lower rotational entropy as a result of its C_2 spatial symmetry.

For $(\text{CH}_3\text{COOH})(\text{H}_2\text{SO}_4)_2$, we located six low-lying energy isomers. As shown in Figure 3, the I-a isomer obviously has the lowest electronic energy and free energy of cluster formation and there is no other isomer within 2 kcal mol⁻¹ in electronic energy. The I-a structure is based on the I-d (C_1) dimer (Figure 2), with an acetic acid bound to the remaining free hydroxyl group (or acidic proton) and oxygen atom. The similar derived performances can be found in other isomers, such as the I-b isomer is based on the I-a (C_1) dimer (Figure 2), and the I-c isomer is based on the I-c (C_2) dimer (Figure 2), and the I-d isomer is based on the I-b (C_i) dimer (Figure 2). The primary hydrogen bonds between the free hydroxyl group of sulfuric acid and the acceptor acetic acid are strong in these structures, characterized by short hydrogen bond lengths and angles approaching linearity.³¹ Generally, the addition of acetic acid molecule to the sulfuric acid dimer allows the formation of multibridding hydrogen bonds. Except for the I-e isomer, the additional hydrogen bond between the acidic proton of sulfuric acid and acetic acid has a short distance (1.34–1.54 Å) compared to the hydrogen bonds in the unhydrated dimer.

Figure 4 displays seven $(\text{CH}_3\text{COOH})(\text{H}_2\text{SO}_4)_2(\text{H}_2\text{O})$ isomers. Structures I-a and I-b are the most stable in terms of electronic energy at 0 K and free energy of cluster formation at 298.15 K, respectively. The I-b isomer is based on the I-a trimer (Figure 3), and the I-c isomer is based on the I-c trimer

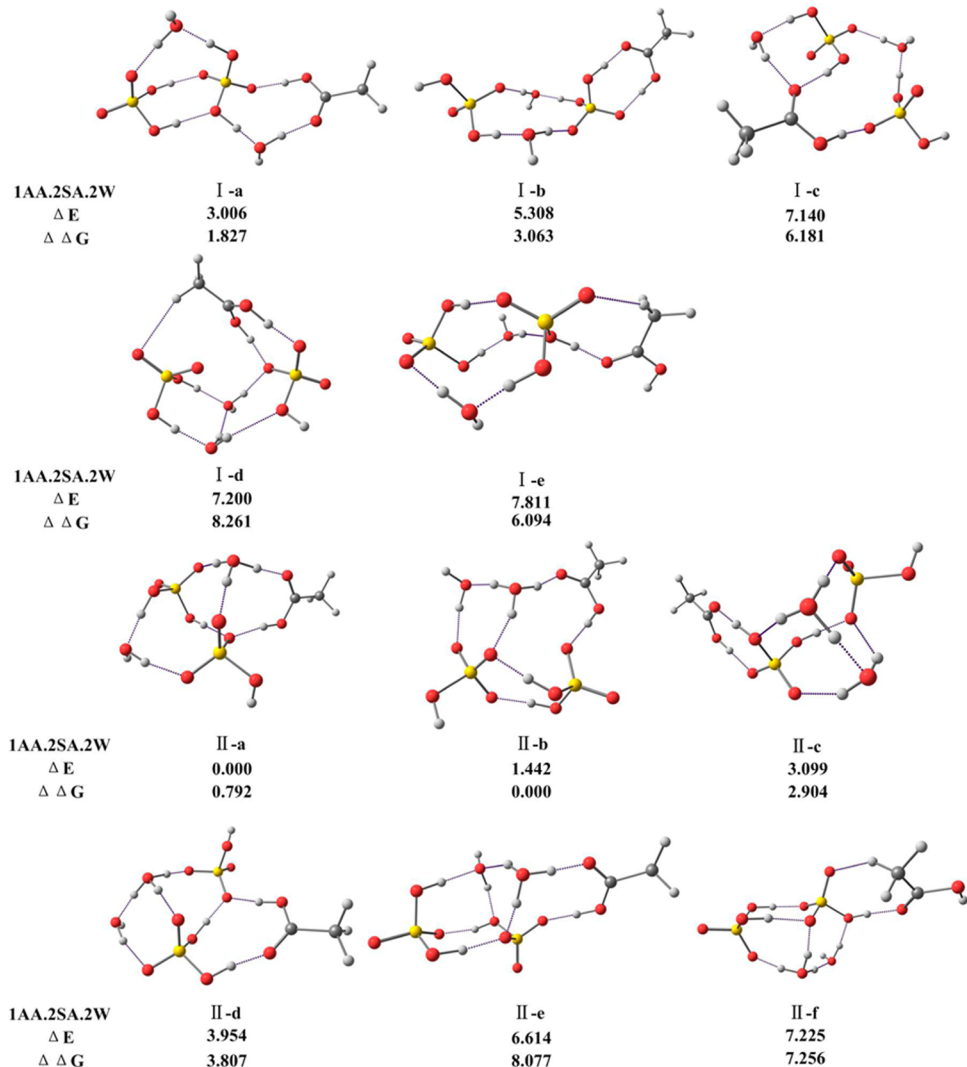


Figure 5. Optimized geometries of $(\text{CH}_3\text{COOH})(\text{H}_2\text{SO}_4)_2(\text{H}_2\text{O})_2$ (1AA.2SA.2W) at the PW91PW91/6-311++G(3df,3pd), ordered by state of dissociation (I, II, III) and increasing ΔE . ΔE represents the relative electronic energy to the global minimum at a standard state of 0 K and 1 atm, and $\Delta \Delta G$ represents the relative free energy of cluster formation to the global minimum at a standard state of 298.15 K and 1 atm.

(Figure 3). Both isomers have the acetic/sulfuric acid trimer structure disrupted by a single donor–single acceptor water molecule bridging the two sulfuric acids. The I-a isomer consists of the $(\text{H}_2\text{SO}_4)_2$ dimer structure I-a (C_1) (Figure 2), with a water bound to the remaining free hydroxyl group of the sulfuric acid and a acetic acid serving as a single donor–double acceptor to bridge the sulfuric acids and water. Structure I-d allows for an interesting perspective on the methods used in this study, and it can be constructed from the $(\text{H}_2\text{SO}_4)_2$ dimer I-d (C_1), merely by adding water and acetic acid molecules in obvious places. One of the lowest energy isomers is diionic structure (the bisulfate anion HSO_4^- , the hydronium cation H_3O^+ , an undissociated sulfuric acid, and an acetic acid). The structure II-a, although not the global minimum, illustrates that the first deprotonation of sulfuric acid can begin even only one water molecule is added.

The 11 lowest energy structures for the $(\text{CH}_3\text{COOH})(\text{H}_2\text{SO}_4)_2(\text{H}_2\text{O})_2$ cluster are displayed in Figure 5. Six of the lowest energy isomers are diionic structures. The lowest electronic energy structure is obviously the diionic structure II-a in which the three bisulfate oxygens accept four hydrogen bonds from the acetic acid, the sulfuric acid, the hydronium, and the

water. In terms of free energy of cluster formation, the structure II-b is the minimum energy structure, which can be thought of as the $(\text{H}_2\text{SO}_4)_2$ dimer I-d (C_1) (Figure 2) with a water, a hydronium and an acetic acid donating three hydrogen bonds to its bottom. Structures I-a, I-b, and I-c have a similar configuration with two water molecules connecting sulfuric acid to acetic acid or another one. Both neutral and diionic isomers have a new structural motif that hydrogen bond also can emerge between methyl group and free oxygen atom of sulfuric acid, though the structures I-d, I-e, and II-f have much higher energy than the minimum.

For the $(\text{CH}_3\text{COOH})(\text{H}_2\text{SO}_4)_2(\text{H}_2\text{O})_3$ system, we found the two neutral isomers, seven diionic isomers, and a tetraionic isomer shown in Figure 6. The tetraionic isomer means that both sulfuric acid molecules have dissociated to two bisulfate and two hydronium ions. The lowest electronic energy structure, II-a, can be thought of as the II-b isomer (Figure 5), the lowest free energy minimum of cluster formation, with an extra water serving as a single acceptor-double donor to the hydronium and oxygen atom of acids, respectively, which making the structure look more like a cage. As for the free energy of cluster formation, the minimum, II-b, only has a network of eight hydrogen bonds

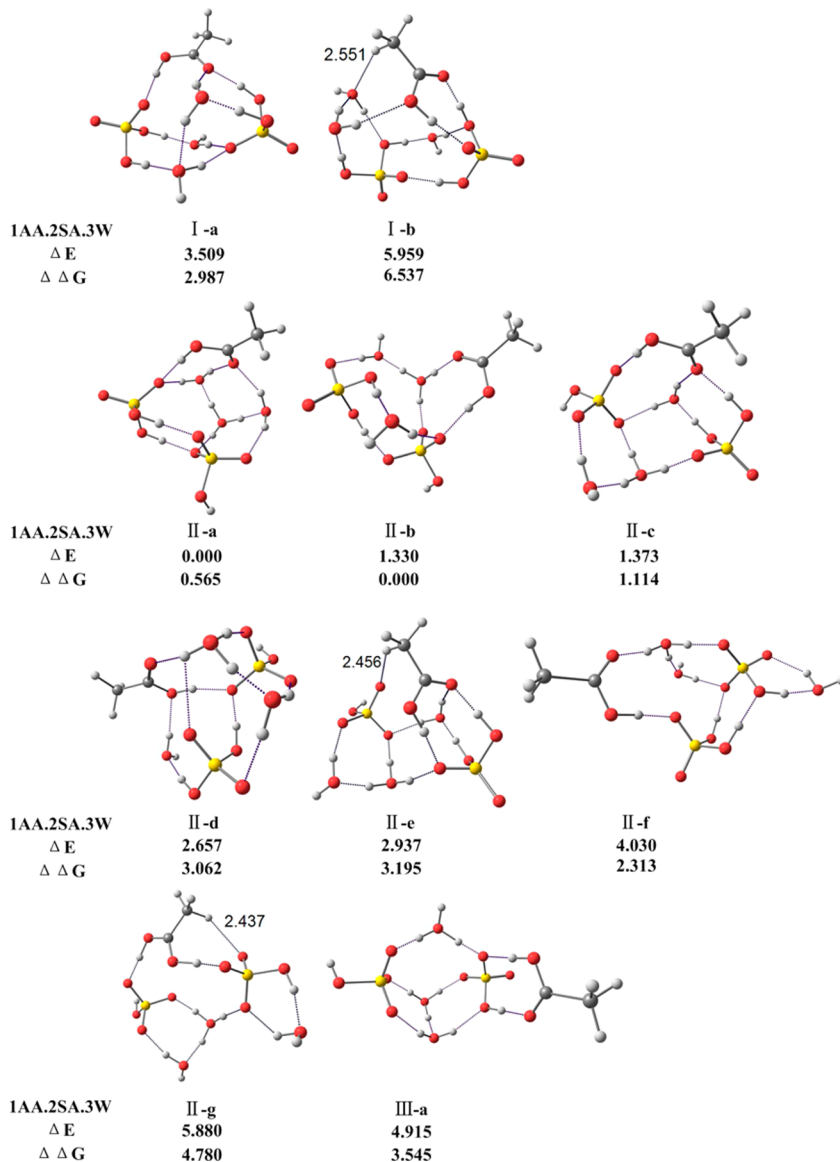


Figure 6. Optimized geometries of $(\text{CH}_3\text{COOH})(\text{H}_2\text{SO}_4)_2(\text{H}_2\text{O})_3$ (1AA.2SA.3W) at the PW91PW91/6-311++G(3df,3pd) level, ordered by state of dissociation (I, II, III) and increasing ΔE . ΔE represents the relative electronic energy to the global minimum at a standard state of 0 K and 1 atm, and $\Delta \Delta G$ represents the relative free energy of cluster formation to the global minimum at a standard state of 298.15 K and 1 atm.

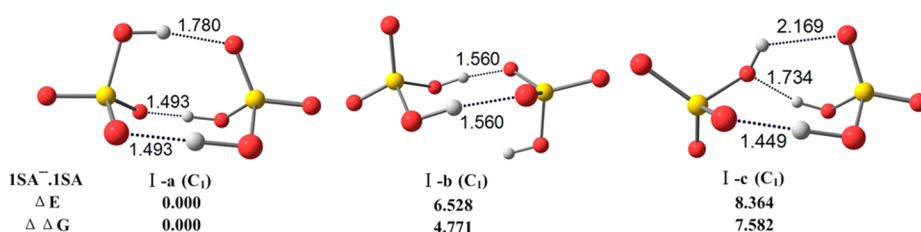


Figure 7. Optimized geometries of $(\text{HSO}_4^-)_2(\text{H}_2\text{SO}_4)$ (1SA-.1SA) at the PW91PW91/6-311++G (3df,3pd) level, ordered by increasing ΔE . ΔE represents the relative electronic energy to the global minimum at a standard state of 0 K and 1 atm, and $\Delta \Delta G$ represents the relative free energy of cluster formation to the global minimum at a standard state of 298.15 K and 1 atm.

while the other structures have a network of nine (I-a, II-c, II-f, II-g, III-a) or ten (I-b, II-a, II-d, II-e) hydrogen bonds. The II-b isomer can be thought as the II-a isomer (Figure 5), the lowest electronic energy minimum, with an extra water to update the network of the structure. The tetraionic structure III-a, although much higher in energy than the minimum, demonstrates a new structural pattern that emerges as more waters are added.

In this structure, the water and the hydroniums are inserted between the bisulfates, bridging the two anions. There are no hydrogen bonds between the bisulfates while there are two hydrogen bonds between the acetic acid and one bisulfate, and this configuration provides charge separation thereby minimizing the electrostatic repulsion between the bisulfate anions as well as the hydroniums. Moreover, both of neutral (I-b) and

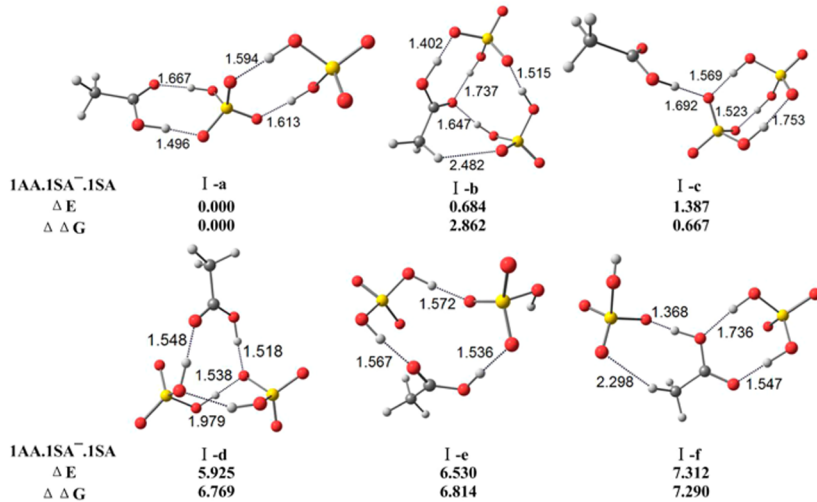


Figure 8. Optimized geometries of $(\text{CH}_3\text{COOH})(\text{HSO}_4^-)(\text{H}_2\text{SO}_4)$ (1AA.1SA⁻.1SA) at the PW91PW91/6-311++G(3df,3pd) level, ordered by increasing ΔE . ΔE represents the relative electronic energy to the global minimum at a standard state of 0 K and 1 atm, and $\Delta\Delta G$ represents the relative free energy of cluster formation to the global minimum at a standard state of 298.15 K and 1 atm.

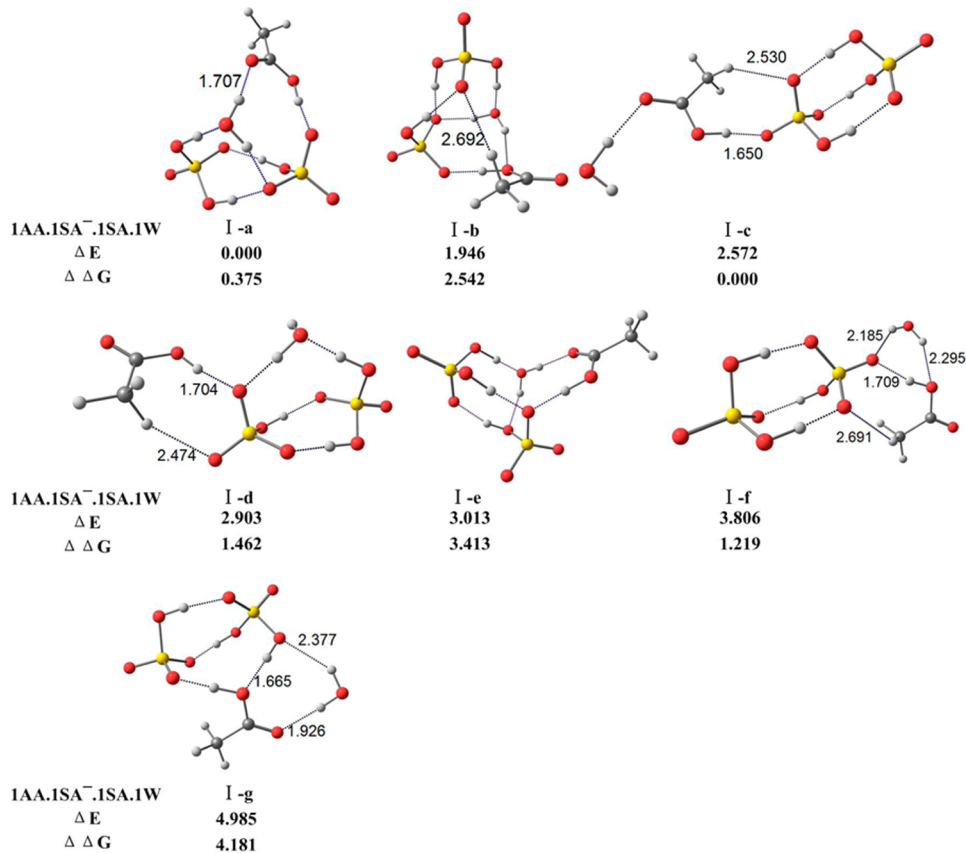


Figure 9. Optimized geometries of $(\text{CH}_3\text{COOH})(\text{HSO}_4^-)(\text{H}_2\text{SO}_4)(\text{H}_2\text{O})$ (1AA.1SA⁻.1SA.1W) at the PW91PW91/6-311++G(3df,3pd) level, ordered by increasing ΔE . ΔE represents the relative electronic energy to the global minimum at a standard state of 0 K and 1 atm, and $\Delta\Delta G$ represents the relative free energy of cluster formation to the global minimum at a standard state of 298.15 K and 1 atm.

dionic (II-e, II-g) isomers have the hydrogen bond between methyl group and free oxygen atom of sulfuric acid, displaying the pattern may exist as more waters were added. Particularly, for the II-e isomer, the gap in electronic energy from the minimum seems much smaller compared with that in II-f (Figure 5).

Some interesting changes can be found if we replace one of the sulfuric acids with a bisulfate anion. As shown in Figure 7, the anion dimers, $(\text{HSO}_4^-)(\text{H}_2\text{SO}_4)$, have three isomers consisting of

cis-H₂SO₄ and bisulfate, and all of them have C_1 symmetry. Unlike isomers in the sulfuric acid dimers, structure I-a (C_1) is an obvious global minimum in electronic energy and free energy of cluster formation due to three strong hydrogen bonds consuming all of the free hydroxyl groups. The isomer I-b (C_1) only has two strong hydrogen bonds. Although the isomer I-c (C_1) have three hydrogen bonds, two of them are weaker OH \cdots OH interactions, as opposed to the stronger OH \cdots O bonds found in I-a (C_1).

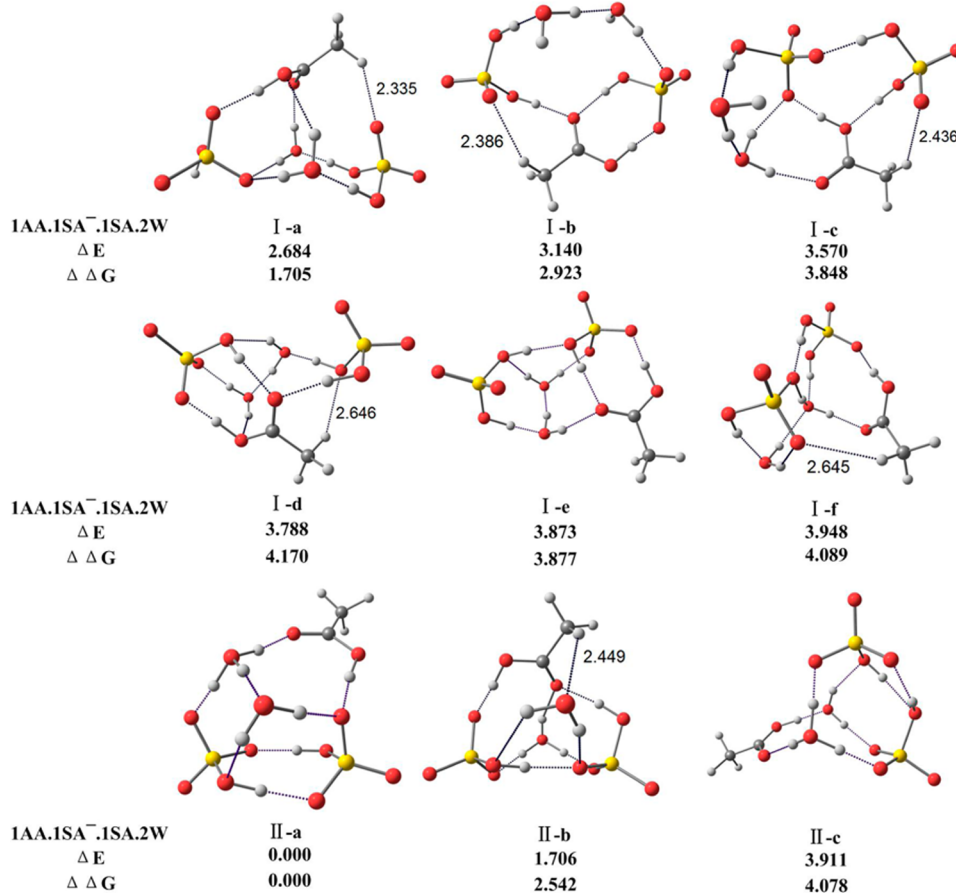


Figure 10. Optimized geometries of $(\text{CH}_3\text{COOH})(\text{HSO}_4^-)(\text{H}_2\text{SO}_4)(\text{H}_2\text{O})_2$ (IAA.1SA⁻.1SA.2W) at the PW91PW91/6-311++G(3df,3pd) level, ordered by state of dissociation (I, II, III) and increasing ΔE . ΔE represents the relative electronic energy to the global minimum at a standard state of 0 K and 1 atm, and $\Delta \Delta G$ represents the relative free energy of cluster formation to the global minimum at a standard state of 298.15 K and 1 atm.

For $(\text{CH}_3\text{COOH})(\text{HSO}_4^-)(\text{H}_2\text{SO}_4)$, we located six low-lying energy isomers. As Figure 8 displays, the I-a isomer, the lowest in electronic energy and free energy of cluster formation, is based on the I-b (C_1) dimer (Figure 7), with an acetic acid bound to the remaining free hydroxyl group and oxygen atom of sulfuric acid. The I-b isomer, within 0.7 kcal mol⁻¹ of the electronic energy minimum, already has a hydrogen bond between methyl group and free oxygen atom of sulfuric acid, even no water is added and much earlier than that in $(\text{CH}_3\text{COOH})(\text{H}_2\text{SO}_4)_2(\text{H}_2\text{O})$ clusters (Figure 4). The I-c isomer is based on the I-a (C_1) dimer (Figure 7), with an acetic acid serving as a single donor to the bisulfate. The I-f isomer shows that the hydrogen bond can emerge between methyl group and free oxygen atom of bisulfate as well.

Figure 9 shows seven $(\text{CH}_3\text{COOH})(\text{HSO}_4^-)(\text{H}_2\text{SO}_4)(\text{H}_2\text{O})$ isomers. It is interesting to find that the configuration between sulfuric acid and bisulfate in the I-a isomer is different from that in the $(\text{HSO}_4^-)(\text{H}_2\text{SO}_4)$ dimer (Figure 7). The hydrogen bond between methyl group and free oxygen atom of sulfuric acid can be found in the I-b isomer while the hydrogen bond between methyl group and free oxygen atom of bisulfate appears in structures I-c, I-d, and I-f, especially the I-c isomer is the lowest in the free energy of cluster formation. Comparing with the $(\text{CH}_3\text{COOH})(\text{H}_2\text{SO}_4)_2(\text{H}_2\text{O})$ clusters (Figure 4), we can find that no deprotonation appears as the first water is added.

The nine low-lying energy structures for the $(\text{CH}_3\text{COOH})(\text{HSO}_4^-)(\text{H}_2\text{SO}_4)(\text{H}_2\text{O})_2$ clusters are displayed in Figure 10.

Three of the lowest energy isomers are triionic structures (two bisulfate anions HSO_4^- , the hydronium cation H_3O^+ , and a water molecule). Structure II-a is obviously the lowest minimum in electronic energy and free energy of cluster formation, and it is based on the I-a isomer (Figure 9), with second water serving as a single acceptor-double donor to the newly formed hydronium and two bisulfates. The structure II-b shows that the hydrogen bond can emerge between methyl group and oxygen atom of water, which may provide more possibility to built cage structure. The hydrogen bond also can be found between methyl group and oxygen of sulfuric acid (I-a, I-b, I-c, I-d), or between methyl group and oxygen of bisulfate (I-f).

For the $(\text{CH}_3\text{COOH})(\text{HSO}_4^-)(\text{H}_2\text{SO}_4)(\text{H}_2\text{O})_3$ systems, we found six neutral and three triionic isomers shown in Figure 11. Isomer I-a is obviously the lowest in electronic energy and free energy of cluster formation, and three water molecules stay together, bridging with sulfuric acid and bisulfate, to build a cage of the structure. Unlike the trend of structural evolution of $(\text{CH}_3\text{COOH})(\text{H}_2\text{SO}_4)_2(\text{H}_2\text{O})_3$ clusters, the second hydronium is not found and the triionic isomers are higher in electronic energy than that of I-a. The replacement of sulfuric acid with bisulfate seems to have an impact on the evolution of acetic/sulfuric acid–water clusters. The hydrogen bond can be found between methyl group and oxygen of water (I-b, I-e, I-f), between methyl group and oxygen of sulfuric acid (I-c), and between methyl group and oxygen of bisulfate (II-a). These configurations can help the isomers to built compact cages, preparing for growth as more water molecules are added.

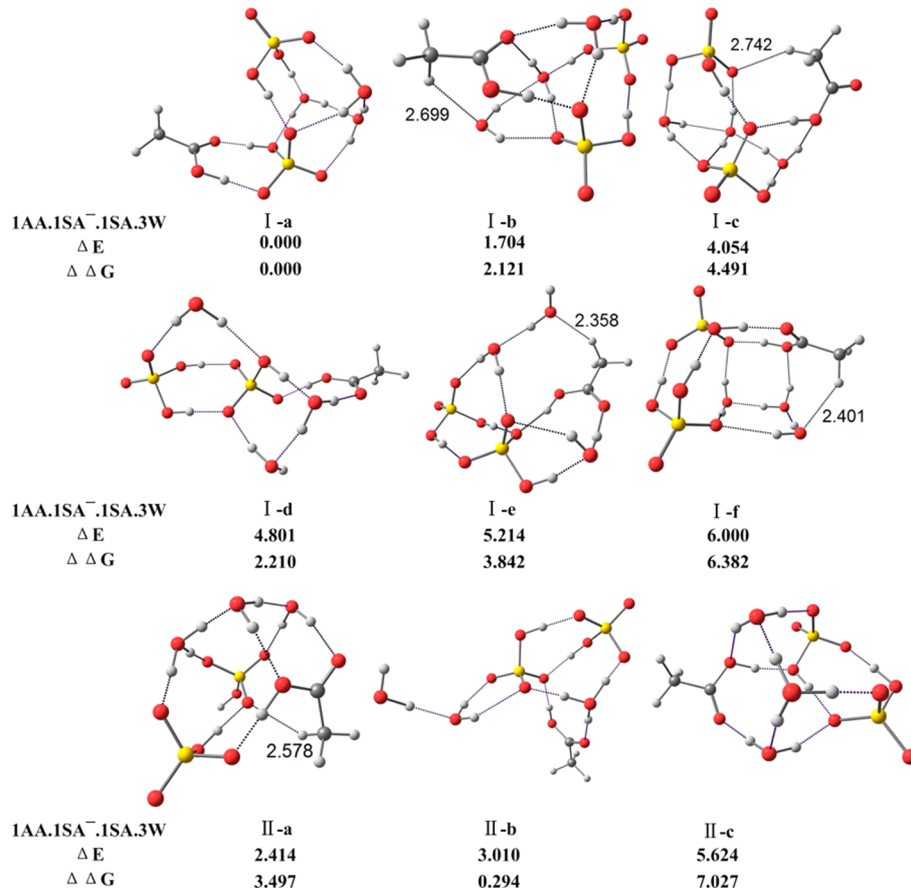


Figure 11. Optimized geometries of $(\text{CH}_3\text{COOH})(\text{HSO}_4^-)(\text{H}_2\text{SO}_4)(\text{H}_2\text{O})_3$ (1AA.1SA⁻.1SA.3W) at the PW91PW91/6-311++G(3df, 3pd) level, ordered by state of dissociation (I, II, III) and increasing ΔE . ΔE represents the relative electronic energy to the global minimum at a standard state of 0 K and 1 atm, and $\Delta \Delta G$ represents the relative free energy of cluster formation to the global minimum at a standard state of 298.15 K and 1 atm.

Table 1. Binding Energies for $(\text{H}_2\text{SO}_4)_2$ and $(\text{CH}_3\text{COOH})(\text{H}_2\text{SO}_4)_2$ at the PW91PW91/6-311++G (3df,3pd) Level

<i>n</i>	isomer	0 K			298.15 K		
		ΔE (kcal mol ⁻¹)	ΔH (kcal mol ⁻¹)	ΔG (kcal mol ⁻¹)	ΔE (kcal mol ⁻¹)	ΔH (kcal mol ⁻¹)	ΔG (kcal mol ⁻¹)
<i>i</i>	I-a	-16.78	-17.12	-5.55	-7.14	-7.72	2.29
<i>i</i>	I-b	-16.60	-16.72	-6.74/-6.74^a	-7.08	-7.39	-0.52/-0.52^a
<i>i</i>	I-c	-16.47	-16.55	-6.39	-4.26	-4.56	2.68
<i>i</i>	I-d	-16.13	-16.52	-4.81	-3.59	-4.17	4.66
<i>ii</i>	I-a	-18.89	-19.15	-6.28/-8.19^a	-3.44	-3.72	4.51
<i>ii</i>	I-b	-15.99	-15.77	-4.30	-2.21	-2.60	5.35
<i>ii</i>	I-c	-14.42	-14.30	-3.09			
<i>ii</i>	I-d	-14.38	-14.34	-2.00			
<i>ii</i>	I-e	-12.41	-12.22	-0.55			
<i>ii</i>	I-f	-11.42	-10.87	-0.29			

^aThe changes in the free energy are calculated via the structural evolution: the product is the global minimum in order of increasing free energy, the reactant is the local (or global) minimum which is fit for the trend of structural evolution, and the changes in free energy are defined as the difference between product and reactant. Global minima are shown in bold.

4.2. Acid Dissociation. Water plays an important role in a lot of processes including acid dissociation.⁷⁷ The dissociation of hydrated sulfuric acids moiety into hydrated ionic species has appealed to many researchers. Sulfuric acid, as a strong acid, completely dissociates in aqueous solutions, even deprotonation

Table 2. Binding Energies for $(\text{CH}_3\text{COOH})(\text{H}_2\text{SO}_4)_2(\text{H}_2\text{O})$ at the PW91PW91/6-311++G (3df,3pd) Level

<i>n</i>	isomer	0 K			298.15 K		
		ΔE (kcal mol ⁻¹)	ΔH (kcal mol ⁻¹)	ΔG (kcal mol ⁻¹)	ΔE (kcal mol ⁻¹)	ΔH (kcal mol ⁻¹)	ΔG (kcal mol ⁻¹)
1	I-a	-7.14	-7.72	2.29	-7.14	-7.72	2.29
1	I-b	-7.08	-7.39	-0.52/-0.52^a	-7.08	-7.39	-0.52/-0.52^a
1	I-c	-4.26	-4.56	2.68	-4.26	-4.56	2.68
1	I-d	-3.59	-4.17	4.66	-3.59	-4.17	4.66
1	I-e	-3.44	-3.72	4.51	-3.44	-3.72	4.51
1	I-f	-2.21	-2.60	5.35	-2.21	-2.60	5.35
1	II-a	-5.60	-6.04	2.47	-5.60	-6.04	2.47

^aThe changes in the free energy are calculated via the structural evolution: the product is the global minimum in order of increasing free energy, the reactant is the local (or global) minimum which is fit for the trend of structural evolution, and the changes in free energy are defined as the difference between product and reactant. Global minima are shown in bold.

in the gas phase happens in the presence of a few waters. The recent review of hydrated acid clusters from Leopold demonstrated that the strong monoprotic acids generally need three to five water molecules before the lowest energy compound contains the ionized acid, and the relative stability of the neutral and ionic species is related to a delicate balance between proton transfer energy, Coulombic attraction, and hydrogen-bond stabilization.³¹ Some experiments on the aggregation-induced acid dissociation of $\text{HCl}(\text{H}_2\text{O})_n$ propose

Table 3. Binding Energies for $(\text{CH}_3\text{COOH})(\text{H}_2\text{SO}_4)_2(\text{H}_2\text{O})_2$ at the PW91PW91/6-311++G (3df,3pd) Level

<i>n</i>	isomer	0 K			298.15 K		
		ΔE (kcal mol ⁻¹)	ΔH (kcal mol ⁻¹)	ΔG (kcal mol ⁻¹)	ΔE (kcal mol ⁻¹)	ΔH (kcal mol ⁻¹)	ΔG (kcal mol ⁻¹)
2	I-a	-10.30	-11.15	-0.46			
2	I-b	-8.00	-8.40	0.77			
2	I-c	-6.16	-6.63	3.89			
2	I-d	-6.10	-6.81	5.97			
2	I-e	-5.49	-6.07	3.80			
2	II-a	-13.30	-14.36	-1.50			
2	II-b	-11.86	-12.63	-2.29/-5.10^a			
2	II-c	-10.20	-11.22	0.61			
2	II-d	-9.35	-10.22	1.52			
2	II-e	-6.69	-8.12	5.79			
2	II-f	-6.08	-7.23	4.96			

^aThe changes in the free energy are calculated via the structural evolution: the product is the global minimum in order of increasing free energy, the reactant is the local (or global) minimum which is fit for the trend of structural evolution, and the changes in free energy are defined as the difference between product and reactant. Global minima are shown in bold.

Table 4. Binding Energies for $(\text{CH}_3\text{COOH})(\text{H}_2\text{SO}_4)_2(\text{H}_2\text{O})_3$ at the PW91PW91/6-311++G (3df,3pd) Level

<i>n</i>	isomer	0 K			298.15 K		
		ΔE (kcal mol ⁻¹)	ΔH (kcal mol ⁻¹)	ΔG (kcal mol ⁻¹)	ΔE (kcal mol ⁻¹)	ΔH (kcal mol ⁻¹)	ΔG (kcal mol ⁻¹)
3	I-a	-6.07	-6.69	3.67			
3	I-b	-3.62	-4.42	7.22			
3	II-a	-9.58	-10.65	1.25			
3	II-b	-8.25	-8.78	+0.69/-0.11^a			
3	II-c	-8.21	-9.14	1.80			
3	II-d	-6.92	-7.58	3.75			
3	II-e	-6.64	-7.64	3.88			
3	II-f	-5.55	-6.19	3.00			
3	II-g	-3.70	-4.29	5.47			
3	III-a	-4.67	-5.72	4.23			

^aThe changes in the free energy are calculated via the structural evolution: the product is the global minimum in order of increasing free energy, the reactant is the local (or global) minimum which is fit for the trend of structural evolution, and the changes in free energy are defined as the difference between product and reactant. Global minima are shown in bold.

a mechanism for the proton transfer process.^{78–80} In addition, Temelso and Shields predicted the first deprotonation of sulfuric acid as a function of temperature for $(\text{H}_2\text{SO}_4)_2(\text{H}_2\text{O})_n$ clusters.⁷

Since acid dissociation at a molecular level seems to be of great interest, we pay an attention on the dissociation of hydrated sulfuric acids compounded with acetic acid. As a significant fraction of organic acid existing in the atmosphere, acetic acid is a weak monoprotic acid and the liquid acetic acid is a hydrophilic (polar) protic solvent, similar to ethanol and water. Our results provide a picture of the first deprotonation of sulfuric acid in terms of electronic energy (E_e) at 0 K and Gibbs free energy of cluster formation (ΔG) at 298.15 K for a system consisting of two sulfuric acid molecules, a single acetic acid molecule and up to three waters (Figure 12). At 0 K, the first deprotonation emerges since first water is added to the trimer, $(\text{CH}_3\text{COOH})(\text{H}_2\text{SO}_4)_2$, but the completely neutral moieties seem to be more stable. Addition of a second water results in deprotonation of most of the clusters, with the diionic species

Table 5. Binding Energies for $(\text{HSO}_4^-)(\text{H}_2\text{SO}_4)$ and $(\text{CH}_3\text{COOH})(\text{HSO}_4^-)(\text{H}_2\text{SO}_4)$ at the PW91PW91/6-311++G(3df,3pd) Level

<i>n</i>	isomer	0 K			298.15 K		
		ΔE (kcal mol ⁻¹)	ΔH (kcal mol ⁻¹)	ΔG (kcal mol ⁻¹)	ΔE (kcal mol ⁻¹)	ΔH (kcal mol ⁻¹)	ΔG (kcal mol ⁻¹)
<i>i</i>	I-a	-46.02	-46.97	-33.28/-33.28^a			
<i>i</i>	I-b	-39.49	-39.86	-28.51			
<i>i</i>	I-c	-37.66	-38.27	-25.70			
<i>ii</i>	I-a	-10.63	-10.63	-0.98/-5.75^a			
<i>ii</i>	I-b	-9.95	-9.80	1.89			
<i>ii</i>	I-c	-9.25	-8.65	-0.31			
<i>ii</i>	I-d	-4.71	-4.18	5.79			
<i>ii</i>	I-e	-4.10	-3.31	5.84			
<i>ii</i>	I-f	-3.32	-2.60	6.31			

^aThe changes in the free energy are calculated via the structural evolution: the product is the global minimum in order of increasing free energy, the reactant is the local (or global) minimum which is fit for the trend of structural evolution, and the changes in free energy are defined as the difference between product and reactant. Global minima are shown in bold.

Table 6. Binding Energies for $(\text{CH}_3\text{COOH})(\text{HSO}_4^-)(\text{H}_2\text{SO}_4)-(\text{H}_2\text{O})$ at the PW91PW91/6-311++G(3df,3pd) Level

<i>n</i>	isomer	0 K			298.15 K		
		ΔE (kcal mol ⁻¹)	ΔH (kcal mol ⁻¹)	ΔG (kcal mol ⁻¹)	ΔE (kcal mol ⁻¹)	ΔH (kcal mol ⁻¹)	ΔG (kcal mol ⁻¹)
1	I-a	-12.04	-13.04	-1.24			
1	I-b	-10.09	-11.01	0.93			
1	I-c	-9.46	-9.55	-1.61/-1.61^a			
1	I-d	-9.13	-9.67	-0.15			
1	I-e	-9.02	-9.95	1.80			
1	I-f	-8.23	-8.15	-0.39			
1	I-g	-7.05	-7.38	2.57			

^aThe changes in the free energy are calculated via the structural evolution: the product is the global minimum in order of increasing free energy, the reactant is the local (or global) minimum which is fit for the trend of structural evolution, and the changes in free energy are defined as the difference between product and reactant. Global minima shown in bold.

Table 7. Binding Energies for $(\text{CH}_3\text{COOH})(\text{HSO}_4^-)(\text{H}_2\text{SO}_4)-(\text{H}_2\text{O})_2$ at the PW91PW91/6-311++G(3df,3pd) Level

<i>n</i>	isomer	0 K			298.15 K		
		ΔE (kcal mol ⁻¹)	ΔH (kcal mol ⁻¹)	ΔG (kcal mol ⁻¹)	ΔE (kcal mol ⁻¹)	ΔH (kcal mol ⁻¹)	ΔG (kcal mol ⁻¹)
2	I-a	-4.60	-4.72	3.70			
2	I-b	-4.14	-4.76	4.92			
2	I-c	-3.71	-4.29	5.84			
2	I-d	-3.49	-4.11	6.16			
2	I-e	-3.41	-4.05	5.87			
2	I-f	-3.33	-3.96	6.08			
2	II-a	-7.28	-8.23	1.99/1.62^a			
2	II-b	-5.58	-6.23	4.53			
2	II-c	-3.37	-4.31	6.07			

^aThe changes in free energy are calculated via the structural evolution: the product is the global minimum in order of increasing free energy, the reactant is the local (or global) minimum which is fit for the trend of structural evolution, and the changes in free energy are defined as the difference between product and reactant. ^bAll energies are in kcal mol⁻¹. Global minima are shown in bold.

more stable than completely neutral moieties. Upon the addition of a third water molecule, the second sulfuric acid also dissociates. For the $(\text{CH}_3\text{COOH})(\text{H}_2\text{SO}_4)_2(\text{H}_2\text{O})_3$ clusters, the

Table 8. Binding Energies for $(\text{CH}_3\text{COOH})(\text{HSO}_4^-)$ - $(\text{H}_2\text{SO}_4)(\text{H}_2\text{O})_3$ at the PW91PW91/6-311++G(3df,3pd) level

<i>n</i>	isomer	0 K		298.15 K	
		ΔE (kcal mol ⁻¹)	ΔH (kcal mol ⁻¹)	ΔG (kcal mol ⁻¹)	
3	I-a	-11.45	-12.12	-2.44	
3	I-b	-9.74	-10.09	-0.32	
3	I-c	-7.39	-7.90	2.05	
3	I-d	-6.65	-6.40	-0.23	
3	I-e	-6.23	-5.95	1.40	
3	I-f	-5.45	-5.63	3.94	
3	II-a	-9.03	-9.82	1.06	
3	II-b	-8.44	-8.27	-2.14	
3	II-c	-5.82	-6.94	4.59	

Global minima are shown in bold.

Table 9. Boltzmann Averaged Binding Energy of the $(\text{CH}_3\text{COOH})(\text{H}_2\text{SO}_4)_2(\text{H}_2\text{O})_n$ and $(\text{CH}_3\text{COOH})(\text{HSO}_4^-)(\text{H}_2\text{SO}_4)(\text{H}_2\text{O})_n$ Clusters at the PW91PW91/6-311++G(3df,3pd) Level

<i>n</i>	0 K		298.15 K	
	ΔE (kcal mol ⁻¹)	ΔH (kcal mol ⁻¹)	ΔG (kcal mol ⁻¹)	
$(\text{CH}_3\text{COOH})(\text{H}_2\text{SO}_4)_2(\text{H}_2\text{O})_{n-1} + \text{H}_2\text{O} \rightarrow (\text{CH}_3\text{COOH})(\text{H}_2\text{SO}_4)_2(\text{H}_2\text{O})_n$				
<i>i</i>	-16.58	-16.84	-6.50	
<i>ii</i>	-18.76	-19.09	-6.05	
1	-7.09	-7.57	-0.38	
2	-13.17	-14.24	-2.12	
3	-9.34	-10.41	1.02	
$(\text{CH}_3\text{COOH})(\text{HSO}_4^-)(\text{H}_2\text{SO}_4)(\text{H}_2\text{O})_{n-1} + \text{H}_2\text{O} \rightarrow (\text{CH}_3\text{COOH})(\text{HSO}_4^-)(\text{H}_2\text{SO}_4)(\text{H}_2\text{O})_n$				
<i>i</i>	-46.02	-46.97	-33.27	
<i>ii</i>	-10.42	-10.38	-0.94	
1	-11.97	-12.97	-1.52	
2	-7.18	-7.93	2.47	
3	-11.34	-12.01	-2.36	

diionic cluster is a few kcal mol⁻¹ more stable than the neutral cluster, which is a few kcal mol⁻¹ more stable than the tetraionic cluster (Figure 12, top). The start of dissociation seems to be delayed at room temperature due to the fact that the free energy of cluster formation becomes positive at one-water level (Figure 12, bottom). The first deprotonation appears and the diionic species is more stable than the undissociated clusters as second water is added. Meanwhile, the addition of a third water seems to be unfavorable at room temperature, though undissociated clusters, diionic and tetraionic species can be found among the lowest isomers of the $(\text{CH}_3\text{COOH})(\text{H}_2\text{SO}_4)_2(\text{H}_2\text{O})_3$ clusters.

Interesting changes have taken place when we replace one of the sulfuric acids with a bisulfate anion (Figure 13). At 0 K, unlike the $(\text{CH}_3\text{COOH})(\text{H}_2\text{SO}_4)_2(\text{H}_2\text{O})$ clusters, the bisulfate anion delays the deprotonation and the first dissociation does not emerge until two waters are added to the $(\text{CH}_3\text{COOH})(\text{HSO}_4^-)(\text{H}_2\text{SO}_4)$ trimer. The diionic species is a few kcal mol⁻¹ more stable than the undissociated clusters containing two water molecules, but the neutral clusters is more favorable than the diionic species due to the addition of a third water. What's more, the second dissociation does not emerge when three waters have been added to the clusters. At room temperature, the growth of clusters seems to be unstable after the dimer, $(\text{HSO}_4^-)(\text{H}_2\text{SO}_4)$, and addition of second water even encounters a positive Gibbs

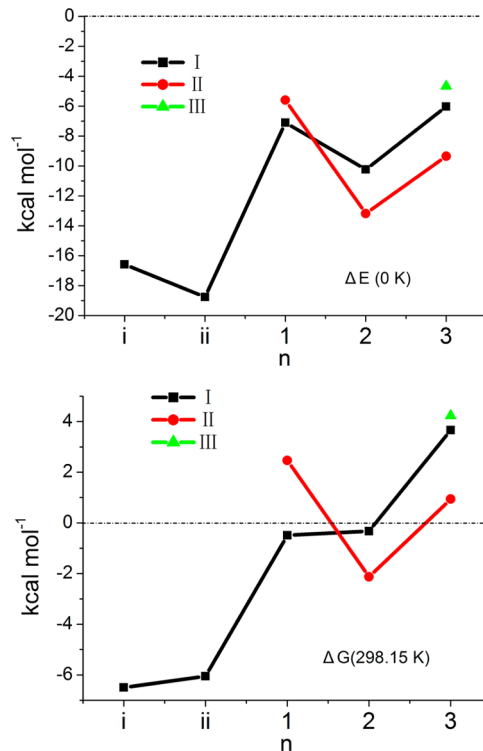


Figure 12. Thermodynamics at the PW91PW91/6-311++G(3df,3pd) level of stepwise $[(\text{CH}_3\text{COOH})(\text{H}_2\text{SO}_4)_2(\text{H}_2\text{O})_{n-1} + \text{H}_2\text{O} \rightarrow (\text{CH}_3\text{COOH})(\text{H}_2\text{SO}_4)_2(\text{H}_2\text{O})_n]$ sulfuric (2)/acetic acid trimer hydrate growth of neutral (I), diionic (II), and tetraionic (III) isomers. The change in energy is defined as the difference between the Boltzmann averaged value for the *n*th of a particular state (I, II, III) and (*n* - 1)th cluster of all the states. *n* = *i* corresponds to $2(\text{H}_2\text{SO}_4) \rightarrow (\text{H}_2\text{SO}_4)_2$, and *n* = *ii* stands for $(\text{H}_2\text{SO}_4)_2 + \text{CH}_3\text{COOH} \rightarrow (\text{CH}_3\text{COOH})(\text{H}_2\text{SO}_4)_2$.

free energy. The clusters become more stable as third water is added, and the neutral clusters are slightly more stable than the diionic species (Figure 13, bottom).

The finding of the growth of hydrated trimer of two sulfuric acid molecules and a single acetic acid at the early stage may have favorable implications for understanding the organics-enhanced nucleation between atmospheric nucleation precursors and acetic acid. By comparison between Figure 12 and Figure 13, we also find that acetic acid and bisulfate anion can promote the hydrated sulfuric acid(s) to form stable structures with different number of water molecules, we predict that the organics-enhanced dissociation and ion-mediated dissociation may play a role at the early stage of the growth of nucleation precursors and their promotions follow a complementary distribution during the process.

4.3. Calculation for the Gibbs Free Energy of Clusters Formation via Structural Evolution. As described in the Methods (more details described in the Supporting Information), the tentative calculation for the Gibbs free energies of the clusters formation is based on the phenomena of structural evolution during the early stage of clusters formation. To focus our attentions on the global minimum at each size of the clusters, we confirm the global minimum of the product first, and then infer the most suitable isomer of the reactant, rather than the opposite order. In terms of the calculations for the Gibbs free energies of clusters formation, no matter the traditional or the tentative, they both describe a possible event in

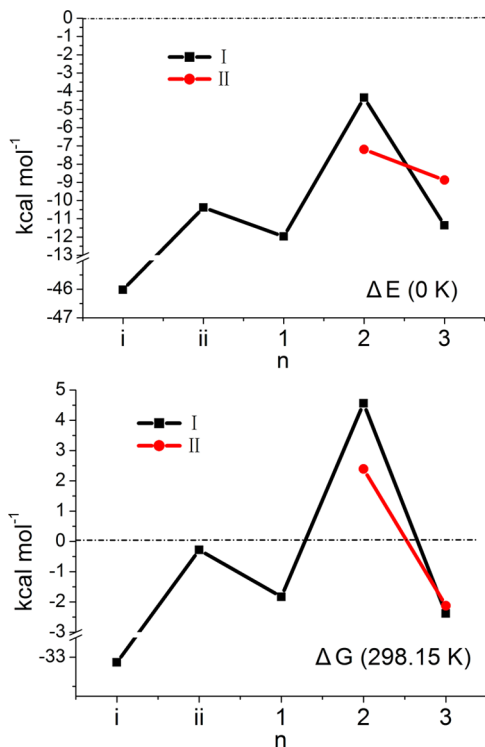


Figure 13. Thermodynamics at the PW91PW91/6-311++G(3df,3pd) level of stepwise $[(\text{CH}_3\text{COOH})(\text{HSO}_4^-)(\text{H}_2\text{SO}_4)(\text{H}_2\text{O})_{n-1} + \text{H}_2\text{O} \rightarrow (\text{CH}_3\text{COOH})(\text{HSO}_4^-)(\text{H}_2\text{SO}_4)(\text{H}_2\text{O})_n]$ bifulfate/sulfuric/acetic acid trimer hydrate growth of neutral (I) and diionic (II) isomers. The change in energy is defined as the difference between the Boltzmann averaged value for the nth cluster of a particular state (I, II) and $(n - 1)$ th cluster of all the states. $n = i$ corresponds to $\text{H}_2\text{SO}_4 + \text{HSO}_4^- \rightarrow (\text{HSO}_4^-)(\text{H}_2\text{SO}_4)$, and $n = ii$ stands for $(\text{HSO}_4^-)(\text{H}_2\text{SO}_4) + \text{CH}_3\text{COOH} \rightarrow (\text{CH}_3\text{COOH})(\text{HSO}_4^-)(\text{H}_2\text{SO}_4)$.

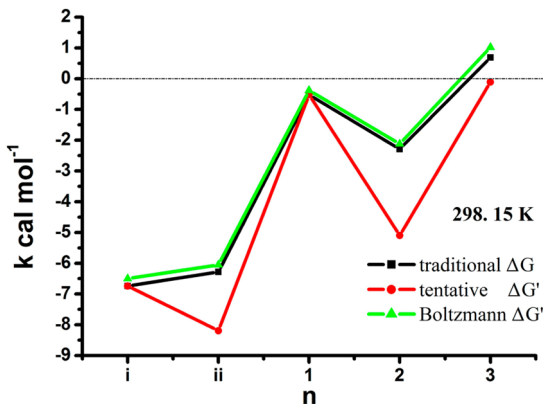


Figure 14. Comparison of three calculation paths for the Gibbs free energies of clusters formation about thermodynamics at the PW91PW91/6-311++G(3df,3pd) level of stepwise $[(\text{CH}_3\text{COOH})(\text{H}_2\text{SO}_4)_2(\text{H}_2\text{O})_{n-1} + \text{H}_2\text{O} \rightarrow (\text{CH}_3\text{COOH})(\text{H}_2\text{SO}_4)_2(\text{H}_2\text{O})_n]$ sulfuric (2)/acetic acid trimer hydrate growth. $n = i$ corresponds to $2(\text{H}_2\text{SO}_4) \rightarrow (\text{H}_2\text{SO}_4)_2$, and $n = ii$ stands for $(\text{H}_2\text{SO}_4)_2 + \text{CH}_3\text{COOH} \rightarrow (\text{CH}_3\text{COOH})(\text{H}_2\text{SO}_4)_2$.

the growth of the $(\text{CH}_3\text{COOH})(\text{H}_2\text{SO}_4)_2(\text{H}_2\text{O})_n$ clusters. To investigate the error limit of the tentative calculation path, we also calculated the Boltzmann averaged binding energies at the PW91PW91/6-311++G(3df,3pd) level of theory for describing the average conditions in the formation of the $(\text{CH}_3\text{COOH})(\text{H}_2\text{SO}_4)_2(\text{H}_2\text{O})_n$ clusters. As shown in Figure 14, the overall

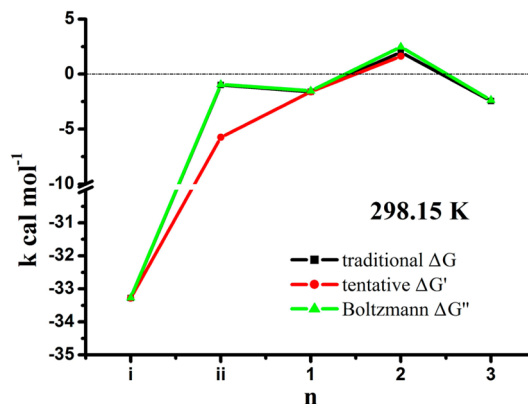


Figure 15. Comparison between three calculation paths for the Gibbs free energies of clusters formation about thermodynamics at the PW91PW91/6-311++G(3df,3pd) level of stepwise $[(\text{CH}_3\text{COOH})(\text{HSO}_4^-)(\text{H}_2\text{SO}_4)(\text{H}_2\text{O})_{n-1} + \text{H}_2\text{O} \rightarrow (\text{CH}_3\text{COOH})(\text{HSO}_4^-)(\text{H}_2\text{SO}_4)(\text{H}_2\text{O})_n]$ bisulfate/sulfuric/acetic acid trimer hydrate growth. $n = i$ corresponds to $\text{H}_2\text{SO}_4 + \text{HSO}_4^- \rightarrow (\text{HSO}_4^-)(\text{H}_2\text{SO}_4)$, and $n = ii$ stands for $(\text{HSO}_4^-)(\text{H}_2\text{SO}_4) + \text{CH}_3\text{COOH} \rightarrow (\text{CH}_3\text{COOH})(\text{HSO}_4^-)(\text{H}_2\text{SO}_4)$.

trends of three lines seem to be consistent with each other and all of them are obtained by using the PW91PW91/6-311++G(3df,3pd) method, which demonstrates that the tentative calculation for the Gibbs free energies of clusters formation is basically feasible. As for the $(\text{CH}_3\text{COOH})(\text{HSO}_4^-)(\text{H}_2\text{SO}_4)(\text{H}_2\text{O})_n$ clusters, the similar comparison of three calculation paths for the Gibbs free energies of clusters formation can be seen in Figure 15. We cautiously predict that the calculation for the Gibbs free energy of clusters formation via the structural evolution can serve as an alternative rationalistic data prepared for experiment research and help to understand the thermodynamics and evolution of the clusters growth.

4.4. Thermodynamics of Clusters Formation. Tables 1-4 contain binding energies, enthalpies, and Gibbs free energies of clusters formation (ΔG) for the $(\text{CH}_3\text{COOH})(\text{H}_2\text{SO}_4)_2(\text{H}_2\text{O})_{n=i,ii,1-3}$ clusters, obtained by the single point electronic energies under the DF-MP2-F12 theory and the thermal corrections under the PW91PW91 correction as described in the Methods. We also add the tentative calculation for ΔG to each global minimum as footnoted in the tables. The dimerization of sulfuric acid is exothermic by 16–17 kcal mol⁻¹, and the trimerization of two sulfuric acids and an acetic acid is exothermic by 11–19 kcal mol⁻¹. For the $(\text{CH}_3\text{COOH})(\text{H}_2\text{SO}_4)_2(\text{H}_2\text{O})_3$ clusters, 8–10 kcal mol⁻¹ is released. Free energies are lower, and some of them are even positive. Viewed from the traditional calculation, they range from -7 kcal mol^{-1} for dimerization of sulfuric acid, to -6 kcal mol^{-1} for trimerization of two sulfuric acids and an acetic acid, to $-0.52 \text{ kcal mol}^{-1}$ for the $(\text{CH}_3\text{COOH})(\text{H}_2\text{SO}_4)_2(\text{H}_2\text{O})$ cluster, to $-2.29 \text{ kcal mol}^{-1}$ for the $(\text{CH}_3\text{COOH})(\text{H}_2\text{SO}_4)_2(\text{H}_2\text{O})_2$ cluster, and to $0.69 \text{ kcal mol}^{-1}$ for the $(\text{CH}_3\text{COOH})(\text{H}_2\text{SO}_4)_2(\text{H}_2\text{O})_3$ cluster, all at room temperature, respectively. In consideration of the tentative calculation, the free energies appear to be more favorable, ranging from -7 kcal mol^{-1} for dimerization of sulfuric acid, to -8 kcal mol^{-1} for trimerization of two sulfuric acids and an acetic acid, to $-0.52 \text{ kcal mol}^{-1}$ for the formation of the $(\text{CH}_3\text{COOH})(\text{H}_2\text{SO}_4)_2(\text{H}_2\text{O})$ cluster, to $-5.10 \text{ kcal mol}^{-1}$ for the $(\text{CH}_3\text{COOH})(\text{H}_2\text{SO}_4)_2(\text{H}_2\text{O})_2$ cluster, and to 0 kcal mol^{-1} for the $(\text{CH}_3\text{COOH})(\text{H}_2\text{SO}_4)_2(\text{H}_2\text{O})_3$ cluster, all at room

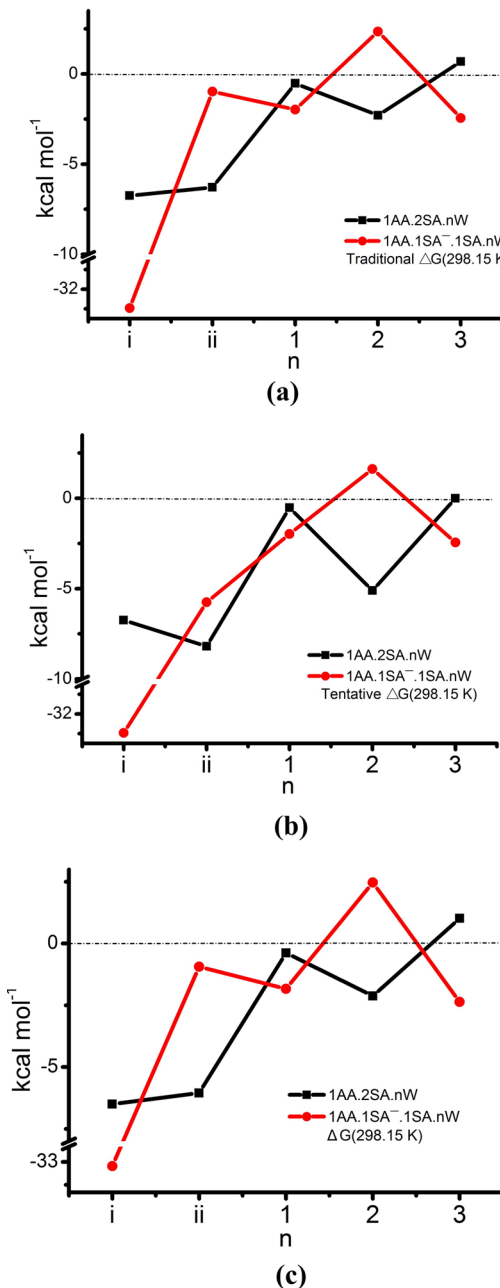


Figure 16. Comparison of thermodynamics at the PW91PW91/6-311+G(3df,3pd) level of stepwise $[T(H_2O)_{n-1} + H_2O \rightarrow T(H_2O)_n]$ (T means trimer) trimer growth between $(CH_3COOH)(H_2SO_4)_2(H_2O)_n$ and $(CH_3COOH)(HSO_4^-)(H_2SO_4)(H_2O)_n$. The change in free energy is defined with three approaches: (a) the traditional calculation; (b) the tentative calculation; (c) the difference between the Boltzmann averaged value for the n th cluster and the $(n - 1)$ th cluster of all state. For the $(CH_3COOH)(H_2SO_4)_2(H_2O)_n$ clusters, $n = i$ corresponds to $2(H_2SO_4) \rightarrow (H_2SO_4)_2$, and $n = ii$ stands for $(H_2SO_4)_2 + CH_3COOH \rightarrow (CH_3COOH)(H_2SO_4)_2$, in terms of the $(CH_3COOH)(HSO_4^-)(H_2SO_4)(H_2O)_n$ clusters, $n = i$ corresponds to $H_2SO_4 + HSO_4^- \rightarrow (HSO_4^-)(H_2SO_4)$, and $n = ii$ stands for $(HSO_4^-)(H_2SO_4) + CH_3COOH \rightarrow (CH_3COOH)(HSO_4^-)(H_2SO_4)$.

temperature, respectively. All of the stepwise free energies are negative at $T = 298.15$ K, though the formation of $(CH_3COOH)(H_2SO_4)_2(H_2O)_3$ from $(CH_3COOH)(H_2SO_4)_2(H_2O)_2$ and a third water still seems to be unfavorable. These results are shown graphically in Figure 14.

Similarly, Tables 5–8 are prepared for the $(CH_3COOH)(HSO_4^-)(H_2SO_4)(H_2O)_{n=i,ii,1-3}$ clusters. The dimerization of sulfuric acid and bisulfate anion is exothermic by 38–47 kcal mol⁻¹, and the formation of the $(CH_3COOH)(HSO_4^-)(H_2SO_4)$ clusters is exothermic by 9–11 kcal mol⁻¹. For the $(CH_3COOH)(HSO_4^-)(H_2SO_4)(H_2O)_3$ clusters, 8–12 kcal mol⁻¹ is released. Actually, free energies are also lower, and some of them are even positive. Viewed from the traditional calculation, they range from -33.28 kcal mol⁻¹ for dimerization of sulfuric acid and bisulfate anion, to -0.98 kcal mol⁻¹ for the formation of the $(CH_3COOH)(HSO_4^-)(H_2SO_4)$ cluster, to -1.97 kcal mol⁻¹ for the $(CH_3COOH)(HSO_4^-)(H_2SO_4)(H_2O)$ cluster, to 2.35 kcal mol⁻¹ for the $(CH_3COOH)(HSO_4^-)(H_2SO_4)(H_2O)_2$ cluster, and to -2.44 kcal mol⁻¹ for the $(CH_3COOH)(HSO_4^-)(H_2SO_4)(H_2O)_3$ cluster, all at room temperature, respectively. In consideration of the tentative calculation, the free energies appear to be more favorable, ranging from -33.28 kcal mol⁻¹ for dimerization of sulfuric acid and bisulfate anion, to -5.75 kcal mol⁻¹ for the $(CH_3COOH)(HSO_4^-)(H_2SO_4)$ cluster, to -1.97 kcal mol⁻¹ for the $(CH_3COOH)(HSO_4^-)(H_2SO_4)(H_2O)$ cluster, to 1.62 kcal mol⁻¹ for the $(CH_3COOH)(HSO_4^-)(H_2SO_4)(H_2O)_2$ cluster, and to -2.44 kcal mol⁻¹ for the $(CH_3COOH)(HSO_4^-)(H_2SO_4)(H_2O)_3$ cluster, all at room temperature, respectively. All of the stepwise free energies are negative, except for the formation of $(CH_3COOH)(HSO_4^-)(H_2SO_4)(H_2O)_2$ from $(CH_3COOH)(HSO_4^-)(H_2SO_4)(H_2O)$ and the second water, at $T = 298.15$ K. These results are shown graphically in Figure 15.

The Boltzmann-averaged energies for the stepwise hydration of two series of clusters (top, $(CH_3COOH)(H_2SO_4)_2(H_2O)_n$; bottom, $(CH_3COOH)(HSO_4^-)(H_2SO_4)(H_2O)_n$) are displayed in Table 9. At room temperature, for the $(CH_3COOH)(H_2SO_4)_2(H_2O)_n$ clusters, the Gibbs free energies range from -6.5 kcal mol⁻¹ for the dimerization to 1 kcal mol⁻¹ for the formation of the $(CH_3COOH)(H_2SO_4)_2(H_2O)_3$ cluster. Clearly, thermodynamics favor the formation of these structures except the $(CH_3COOH)(H_2SO_4)_2(H_2O)_3$ clusters. As for the $(CH_3COOH)(HSO_4^-)(H_2SO_4)(H_2O)_n$ clusters, the Gibbs free energies range from -33 kcal mol⁻¹ for the dimerization to 2 kcal mol for the formation of the $(CH_3COOH)(HSO_4^-)(H_2SO_4)(H_2O)_2$ cluster at 298 K. The formation of the $(CH_3COOH)(HSO_4^-)(H_2SO_4)(H_2O)_3$ cluster seems to be more favorable than that of the $(CH_3COOH)(HSO_4^-)(H_2SO_4)(H_2O)_2$ cluster. These results are shown graphically in Figure 16(c).

4.5. Comparison between the Promotions from Organic Acid and Anion. We do some comparisons of clusters growth between the $(CH_3COOH)(H_2SO_4)_2(H_2O)_n$ clusters and the $(CH_3COOH)(HSO_4^-)(H_2SO_4)(H_2O)_n$ clusters. As Figure 16 shows, the ensemble trends of the three graphs remained unchanged basically, though the change in free energy is defined through three approaches. For the $(CH_3COOH)(H_2SO_4)_2(H_2O)_n$ clusters (the black line), the first two steps seem to be favorable, but the start of hydration is a little difficult. The formation of the $(CH_3COOH)(H_2SO_4)_2(H_2O)_2$ cluster appears to be particularly favorable, while the next step becomes much harder. When we replace one of sulfuric acids with a bisulfate anion, the dimerization of sulfuric acid and bisulfate anion gets a much lower start point (the red line), but the trimerization seems to be a slightly unfavorable. The start of hydration appears to be more favorable than that of the $(CH_3COOH)(H_2SO_4)_2(H_2O)_n$ clusters and the next two steps have diametrically opposite performances compared with that of the $(CH_3COOH)(H_2SO_4)_2(H_2O)_n$ clusters. The growth trend

of the $(\text{CH}_3\text{COOH})(\text{H}_2\text{SO}_4)_2(\text{H}_2\text{O})_n$ clusters seems to be as flexural as that of the $(\text{CH}_3\text{COOH})(\text{HSO}_4^-)(\text{H}_2\text{SO}_4)(\text{H}_2\text{O})_n$ clusters, but the stable structures have different number of water molecules for two series of clusters. The comparisons from Figure 16 demonstrate that the replacement with anion changes the stable configurations at the early stage of the clusters growth and provides supplementary stable precursors at the unfavorable points of the initial clusters. The promotions from ion-mediated mechanism and organics-enhanced mechanism seem to follow a complementary distribution at the early stage of clusters growth.

5. CONCLUSIONS

We investigated the thermodynamics of hydration of $(\text{CH}_3\text{COOH})(\text{H}_2\text{SO}_4)_2$ using high-level DFT calculations, and studied its implication on acid dissociation and clusters growth. We also replace one of the sulfuric acids in the trimer, $(\text{CH}_3\text{COOH})(\text{H}_2\text{SO}_4)_2$, with a bisulfate anion to explore the difference between two series of clusters, and the interaction of the promotions from ion-mediated mechanism and organics-enhanced mechanism. For the two series of clusters, we located the assumed global and many low-lying local minima for each cluster size. For the $(\text{CH}_3\text{COOH})(\text{H}_2\text{SO}_4)_2(\text{H}_2\text{O})_{n=1,ii,1-3}$ clusters, The results in this study supply a picture of the first deprotonation of $(\text{CH}_3\text{COOH})(\text{H}_2\text{SO}_4)_2$ trimer hydrates to form diionic $[(\text{CH}_3\text{COOH})(\text{H}_2\text{SO}_4)(\text{HSO}_4^-)\text{H}_3\text{O}^+](\text{H}_2\text{O})_{n=1}]$ and tetraionic $[(\text{CH}_3\text{COOH})(\text{HSO}_4^-)\text{H}_3\text{O}^+]_2(\text{H}_2\text{O})_{n=2}]$ clusters at 0 and 298.15 K, respectively. At 0 K, the $(\text{CH}_3\text{COOH})(\text{H}_2\text{SO}_4)_2$ trimer undergoes the first acid dissociation of one sulfuric acid after the addition of only one water and both acids after the addition of three waters. At 298.15 K, the $(\text{CH}_3\text{COOH})(\text{H}_2\text{SO}_4)_2$ trimer undergoes the first acid dissociation of one sulfuric acid after the addition of two waters. However, the first acid dissociation of both sulfuric acids seems to be unfavorable before the addition of four waters. In terms of the $(\text{CH}_3\text{COOH})(\text{HSO}_4^-)(\text{H}_2\text{SO}_4)(\text{H}_2\text{O})_{n=1,ii,1-3}$ clusters, the bisulfate anion delays the first acid dissociation of one sulfuric acid to the addition of two waters at 0 K and the addition of three waters at 298.15 K. The first acid dissociation of both sulfuric acids does not appear even at 0 K. From the comparison between two series, we find that the bisulfate anion has an obviously impact on the hydration of the $(\text{CH}_3\text{COOH})(\text{H}_2\text{SO}_4)_2$ trimer, and provides the thermodynamic process with a supplementary performance. It is worthy to take a further study in this aspect. We tentatively predict that the promotions from ion-mediated mechanism and organics-enhanced mechanism follow a complementary distribution at the early stage of clusters growth. Calculation for the Gibbs free energies of clusters formation via the structural evolution is basically feasible through the comparison among three calculation paths. We cautiously predict that it can serve as an alternative rationalistic data prepared for experiment research and help to understand the thermodynamics and evolution of the clusters growth. Certainly, more experiment studies and calculations are needed to further test its utility.

■ ASSOCIATED CONTENT

Supporting Information

Details about the phenomena of the structural evolution during the early stage of the clusters formation, the tentative calculations for the Gibbs free energies of clusters formation via the trend of structural evolution, all the PW91PW91/6-311++G(3df,3pd) optimized Cartesian coordinates, and DF-MP2-F12 single point energies for each isomer. This material is available free of charge via the Internet at <http://pubs.acs.org>.

■ AUTHOR INFORMATION

Corresponding Author

^{*}(W.H.) E-mail: huangwei6@ustc.edu.cn.

Notes

The authors declare no competing financial interest.

■ ACKNOWLEDGMENTS

The study was supported by grants from the National Natural Science Foundation of China (21133008), the Foundation of the Director of Anhui Institute of Optics and Fine Mechanics (Y23H161131), and the “Interdisciplinary and Cooperative Team” of CAS. Acknowledgement is also made to the “Thousand Youth Talents Plan”. Part of the computation was performed at the Supercomputing Center of the Chinese Academy of Sciences and Supercomputing Center of USTC.

■ REFERENCES

- (1) Molina, M. J.; Molina, L. T.; Zhang, R. Y.; Meads, R. F.; Spencer, D. D. The Reaction of ClONO₂ with HCl on Aluminum Oxide. *Geophys. Res. Lett.* **1997**, *24*, 1619–1622.
- (2) Solomon, S.; Qin, D.; Manning, M.; Chen, Z. *Climate Change 2007—the Physical Science Basis: Working Group I Contribution to the Fourth Assessment Report of the Ipcc*; Cambridge University Press: Cambridge, U.K., 2007.
- (3) Zhang, R. Y.; Leu, M. T.; Molina, M. J. Formation of Polar Stratospheric Clouds on Preactivated Background Aerosols. *Geophys. Res. Lett.* **1996**, *23*, 1669–1672.
- (4) Zhang, R. Y.; Li, G. H.; Fan, J. W.; Wu, D. L.; Molina, M. J. Intensification of Pacific Storm Track Linked to Asian Pollution. *Proc. Natl. Acad. Sci. U.S.A.* **2007**, *104*, 5295–5299.
- (5) Zhao, J.; Levitt, N. P.; Zhang, R. Y. Heterogeneous Chemistry of Octanal and 2,4-Hexadienal with Sulfuric Acid. *Geophys. Res. Lett.* **2005**, *32*, L09802.
- (6) Xu, W.; Zhang, R. Theoretical Investigation of Interaction of Dicarboxylic Acids with Common Aerosol Nucleation Precursors. *J. Phys. Chem. A* **2012**, *116*, 4539–4550.
- (7) Temelso, B.; Phan, T. N.; Shields, G. C. Computational Study of the Hydration of Sulfuric Acid Dimers: Implications for Acid Dissociation and Aerosol Formation. *J. Phys. Chem. A* **2012**, *116*, 9745–9758.
- (8) Zhang, R.; Khalizov, A.; Wang, L.; Hu, M.; Xu, W. Nucleation and Growth of Nanoparticles in the Atmosphere. *Chem. Rev.* **2012**, *112*, 1957–2011.
- (9) Zhang, R. Atmospheric Science. Getting to the Critical Nucleus of Aerosol Formation. *Science* **2010**, *328*, 1366–1367.
- (10) Kulmala, M.; Riipinen, I.; Sipila, M.; Manninen, H. E.; Petaja, T.; Junninen, H.; Dal Maso, M.; Mordas, G.; Mirme, A.; Vana, M.; et al. Toward Direct Measurement of Atmospheric Nucleation. *Science* **2007**, *318*, 89–92.
- (11) Sipila, M.; Berndt, T.; Petaja, T.; Brus, D.; Vanhanen, J.; Stratmann, F.; Patokoski, J.; Mauldin, R. L.; Hyvarinen, A. P.; Lihavainen, H.; et al. The Role of Sulfuric Acid in Atmospheric Nucleation. *Science* **2010**, *327*, 1243–1246.
- (12) Jiang, J. K.; Zhao, J.; Chen, M. D.; Eisele, F. L.; Scheckman, J.; Williams, B. J.; Kuang, C. A.; McMurry, P. H. First Measurements of Neutral Atmospheric Cluster and 1–2 Nm Particle Number Size Distributions During Nucleation Events. *Aerosol. Sci. Technol.* **2011**, *45*, II–V.
- (13) Lee, S. H.; Allen, H. C. Analytical Measurements of Atmospheric Urban Aerosol. *Anal. Chem.* **2012**, *84*, 1196–1201.
- (14) Bzdek, B. R.; Johnston, M. V. New Particle Formation and Growth in the Troposphere. *Anal. Chem.* **2010**, *82*, 7871–7878.
- (15) Kirkby, J.; Curtius, J.; Almeida, J.; Dunne, E.; Duplissy, J.; Ehrhart, S.; Franchin, A.; Gagne, S.; Ickes, L.; Kurten, A.; et al. Role of Sulphuric Acid, Ammonia and Galactic Cosmic Rays in Atmospheric Aerosol Nucleation. *Nature* **2011**, *476*, 429–U77.

- (16) Zheng, J.; Khalizov, A.; Wang, L.; Zhang, R. Y. Atmospheric Pressure-Ion Drift Chemical Ionization Mass Spectrometry for Detection of Trace Gas Species. *Anal. Chem.* **2010**, *82*, 7302–7308.
- (17) Zhang, R. Y.; Suh, I.; Zhao, J.; Zhang, D.; Fortner, E. C.; Tie, X. X.; Molina, L. T.; Molina, M. J. Atmospheric New Particle Formation Enhanced by Organic Acids. *Science* **2004**, *304*, 1487–1490.
- (18) Fan, J. W.; Zhang, R. Y.; Collins, D.; Li, G. H. Contribution of Secondary Condensable Organics to New Particle Formation: A Case Study in Houston, Texas. *Geophys. Res. Lett.* **2006**, *33*, L15802.
- (19) Zhang, R. Y.; Wang, L.; Khalizov, A. F.; Zhao, J.; Zheng, J.; McGraw, R. L.; Molina, L. T. Formation of Nanoparticles of Blue Haze Enhanced by Anthropogenic Pollution. *Proc. Natl. Acad. Sci. U.S.A.* **2009**, *106*, 17650–17654.
- (20) Nadykto, A. B.; Yu, F. Q. Strong Hydrogen Bonding between Atmospheric Nucleation Precursors and Common Organics. *Chem. Phys. Lett.* **2007**, *435*, 14–18.
- (21) Zhao, J.; Khalizov, A.; Zhang, R. Y.; McGraw, R. Hydrogen-Bonding Interaction in Molecular Complexes and Clusters of Aerosol Nucleation Precursors. *J. Phys. Chem. A* **2009**, *113*, 680–689.
- (22) Zhao, J.; Zhang, R. Y.; Misawa, K.; Shibuya, K. Experimental Product Study of the OH-Initiated Oxidation of M-Xylene. *J. Photochem. Photobiol., A* **2005**, *176*, 199–207.
- (23) Zhang, D.; Lei, W. F.; Zhang, R. Y. Mechanism of OH Formation from Ozonolysis of Isoprene: Kinetics and Product Yields. *Chem. Phys. Lett.* **2002**, *358*, 171–179.
- (24) Lei, W. F.; Zhang, R. Y. Theoretical Study of Hydroxyisoprene Alkoxy Radicals and Their Decomposition Pathways. *J. Phys. Chem. A* **2001**, *105*, 3808–3815.
- (25) Zhao, J.; Levitt, N. P.; Zhang, R.; Chen, J. Heterogeneous Reactions of Methylglyoxal in Acidic Media: Implications for Secondary Organic Aerosol Formation. *Environ. Sci. Technol.* **2006**, *40*, 7682–7687.
- (26) Zhao, J.; Levitt, N. P.; Zhang, R. Y. Heterogeneous Chemistry of Octanal and 2,4-Hexadienal with Sulfuric Acid. *Geophys. Res. Lett.* **2005**, *32*, L09802.
- (27) McGraw, R.; Zhang, R. Multivariate Analysis of Homogeneous Nucleation Rate Measurements. Nucleation in the P-Toluic Acid/Sulfuric Acid/Water System. *J. Chem. Phys.* **2008**, *128*, 064508.
- (28) Yu, F. Q.; Turco, R. P. Ultrafine Aerosol Formation Via Ion-Mediated Nucleation. *Geophys. Res. Lett.* **2000**, *27*, 883–886.
- (29) Yu, F. From Molecular Clusters to Nanoparticles: Second-Generation Ion-Mediated Nucleation Model. *Atmos. Chem. Phys.* **2006**, *6*, 5193–5211.
- (30) Vaida, V.; Kjaergaard, H. G.; Feierabend, K. J. Hydrated Complexes: Relevance to Atmospheric Chemistry and Climate. *Int. Rev. Phys. Chem.* **2003**, *22*, 203–219.
- (31) Leopold, K. R. Hydrated Acid Clusters. *Annu. Rev. Phys. Chem.* **2011**, *62*, 327–349.
- (32) Kurten, T.; Noppel, M.; Vehkamaki, H.; Salonen, M.; Kulmala, M. Quantum Chemical Studies of Hydrate Formation of H_2SO_4 and HSO_4^- . *Boreal Environ. Res.* **2007**, *12*, 431–453.
- (33) Hanson, D. R.; Eisele, F. Diffusion of H_2SO_4 in Humidified Nitrogen: Hydrated H_2SO_4 . *J. Phys. Chem. A* **2000**, *104*, 1715–1719.
- (34) Temelso, B.; Morrell, T. E.; Shields, R. M.; Allodi, M. A.; Wood, E. K.; Kirschner, K. N.; Castonguay, T. C.; Archer, K. A.; Shields, G. C. Quantum Mechanical Study of Sulfuric Acid Hydration: Atmospheric Implications. *J. Phys. Chem. A* **2012**, *116*, 2209–2224.
- (35) Xu, Y. S.; Nadykto, A. B.; Yu, F. Q.; Jiang, L.; Wang, W. Formation and Properties of Hydrogen-Bonded Complexes of Common Organic Oxalic Acid with Atmospheric Nucleation Precursors. *J. Mol. Struct.: THEOCHEM* **2010**, *951*, 28–33.
- (36) Shields, G. C.; Moran, T. F. Double Electron-Transfer Reactions of CO_2^{2+} Ions. *Chem. Phys. Lett.* **1983**, *101*, 287–290.
- (37) Shields, G. C.; Moran, T. F. Molecular Charge-Transfer Cross-Sections and Their Correlation with Reactant Ion Structures. *J. Phys. Chem.* **1985**, *89*, 4027–4031.
- (38) Shields, G. C.; Moran, T. F. Doubly-Charged Gas-Phase Cations. *Theor. Chim. Acta* **1986**, *69*, 147–159.
- (39) Shields, G. C.; Wennberg, L.; Wilcox, J. B.; Moran, T. F. Sensitivity of Charge-Transfer Reactions to Hydrocarbon Ion Structures. *Org. Mass Spectrom.* **1986**, *21*, 137–149.
- (40) Shields, G. C.; Steiner, P. A.; Nelson, P. R.; Trauner, M. C.; Moran, T. F. Charge-Transfer Reactions of Organic Ions Containing Oxygen - Correlation between Reaction Energetics and Cross-Sections. *Org. Mass Spectrom.* **1987**, *22*, 64–69.
- (41) Pickard, F. C.; Dunn, M. E.; Shields, G. C. Comparison of Model Chemistry and Density Functional Theory Thermochemical Predictions with Experiment for Formation of Ionic Clusters of the Ammonium Cation Complexed with Water and Ammonia; Atmospheric Implications. *J. Phys. Chem. A* **2005**, *109*, 4905–4910.
- (42) Jurema, M. W.; Kirschner, K. N.; Shields, G. C. Modeling of Magic Water Clusters $(\text{H}_2\text{O})_{20}$ and $(\text{H}_2\text{O})_{21}\text{H}^+$ with the PM3 Quantum-Mechanical Method. *J. Comput. Chem.* **1993**, *14*, 1326–1332.
- (43) Morrell, T. E.; Shields, G. C. Atmospheric Implications for Formation of Clusters of Ammonium and 1–10 Water Molecules. *J. Phys. Chem. A* **2010**, *114*, 4266–4271.
- (44) Husar, D. E.; Temelso, B.; Ashworth, A. L.; Shields, G. C. Hydration of the Bisulfate Ion: Atmospheric Implications. *J. Phys. Chem. A* **2012**, *116*, 5151–5163.
- (45) Jurema, M. W.; Shields, G. C. Ability of the Pm3 Quantum-Mechanical Method to Model Intermolecular Hydrogen-Bonding between Neutral Molecules. *J. Comput. Chem.* **1993**, *14*, 89–104.
- (46) Kirschner, K. N.; Sherer, E. C.; Shields, G. C. Use of the Supermolecule Approach to Model the Syn and Anti Conformations of Solvated Cyclic 3',5'-Adenosine Monophosphate. *J. Phys. Chem.* **1996**, *100*, 3293–3298.
- (47) Lively, T. N.; Jurema, M. W.; Shields, G. C. Hydrogen-Bonding of Nucleotide Base-Pairs - Application of the PM3Method. *Int. J. Quantum Chem.* **1994**, *52*, 95–107.
- (48) Kirschner, K. N.; Shields, G. C. Quantum-Mechanical Investigation of Large Water Clusters. *Int. J. Quantum Chem.* **1994**, *5*, 349–360.
- (49) Sherer, E. C.; Turner, G. M.; Lively, T. N.; Landry, D. W.; Shields, G. C. A Semiempirical Transition State Structure for the First Step in the Alkaline Hydrolysis of Cocaine. Comparison between the Transition State Structure, the Phosphonate Monoester Transition State Analog, and a Newly Designed Thiophosphonate Transition State Analog. *J. Mol. Model.* **1996**, *2*, 62–69.
- (50) Sherer, E. C.; Yang, G.; Turner, G. M.; Shields, G. C.; Landry, D. W. Comparison of Experimental and Theoretical Structures of a Transition State Analogue Used for the Induction of Anti-Cocaine Catalytic Antibodies. *J. Phys. Chem. A* **1997**, *101*, 8526–8529.
- (51) Shields, G. C.; Laughton, C. A.; Orozco, M. Molecular Dynamics Simulations of the D(T Center Dot a Center Dot T) Triple Helix. *J. Am. Chem. Soc.* **1997**, *119*, 7463–7469.
- (52) Shields, G. C.; Laughton, C. A.; Orozco, M. Molecular Dynamics Simulation of a PNA Center Dot DNA Center Dot PNA Triple Helix in Aqueous Solution. *J. Am. Chem. Soc.* **1998**, *120*, 5895–5904.
- (53) Sherer, E. C.; Bono, S. J.; Shields, G. C. Further Quantum Mechanical Evidence That Difluorotoluene Does Not Hydrogen Bond. *J. Phys. Chem. B* **2001**, *105*, 8445–8451.
- (54) Kirschner, K. N.; Lexa, K. W.; Salisburg, A. M.; Alser, K. A.; Joseph, L.; Andersen, T. T.; Bennett, J. A.; Jacobson, H. I.; Shields, G. C. Computational Design and Experimental Discovery of an Antiestrogenic Peptide Derived from Alpha-Fetoprotein. *J. Am. Chem. Soc.* **2007**, *129*, 6263–6268.
- (55) Lexa, K. W.; Alser, K. A.; Salisburg, A. M.; Ellens, D. J.; Hernandez, L.; Bono, S. J.; Michael, H. C.; Derby, J. R.; Skiba, J. G.; Feldgus, S.; et al. The Search for Low Energy Conformational Families of Small Peptides: Searching for Active Conformations of Small Peptides in the Absence of a Known Receptor. *Int. J. Quantum Chem.* **2007**, *107*, 3001–3012.
- (56) Shields, G. C.; Kirschner, K. N. The Limitations of Certain Density Functionals in Modeling Neutral Water Clusters. *Synth. React. Inorg., Met.-Org., Nano-Met. Chem.* **2008**, *38*, 32–36.

- (57) Salisburg, A. M.; Deline, A. L.; Lexa, K. W.; Shields, G. C.; Kirschner, K. N. Ramachandran-Type Plots for Glycosidic Linkages: Examples from Molecular Dynamic Simulations Using the Glycam06 Force Field. *J. Comput. Chem.* **2009**, *30*, 910–921.
- (58) Dunn, M. E.; Pokon, E. K.; Shields, G. C. Thermodynamics of Forming Water Clusters at Various Temperatures and Pressures by Gaussian-2, Gaussian-3, Complete Basis Set-Qb3, and Complete Basis Set-Apno Model Chemistries; Implications for Atmospheric Chemistry. *J. Am. Chem. Soc.* **2004**, *126*, 2647–2653.
- (59) Dunn, M. E.; Pokon, E. K.; Shields, G. C. The Ability of the Gaussian-2, Gaussian-3, Complete Basis Set-Qb3, and Complete Basis Set-Apno Model Chemistries to Model the Geometries of Small Water Clusters. *Int. J. Quantum Chem.* **2004**, *100*, 1065–1070.
- (60) Day, M. B.; Kirschner, K. N.; Shields, G. C. Pople's Gaussian-3 Model Chemistry Applied to an Investigation of $(\text{H}_2\text{O})_8$ Water Clusters. *Int. J. Quantum Chem.* **2005**, *102*, 565–572.
- (61) Day, M. B.; Kirschner, K. N.; Shields, G. C. Global Search for Minimum Energy $(\text{H}_2\text{O})_N$ Clusters, $N = 3–5$. *J. Phys. Chem. A* **2005**, *109*, 6773–6778.
- (62) Dunn, M. E.; Evans, T. M.; Kirschner, K. N.; Shields, G. C. Prediction of Accurate Anharmonic Experimental Vibrational Frequencies for Water Clusters, $(\text{H}_2\text{O})_N$, $N = 2–5$. *J. Phys. Chem. A* **2006**, *110*, 303–309.
- (63) Shields, R. M.; Temelso, B.; Archer, K. A.; Morrell, T. E.; Shields, G. C. Accurate Predictions of Water Cluster Formation, $(\text{H}_2\text{O})_{N=2–10}$. *J. Phys. Chem. A* **2010**, *114*, 11725–11737.
- (64) Temelso, B.; Archer, K. A.; Shields, G. C. Benchmark Structures and Binding Energies of Small Water Clusters with Anharmonicity Corrections. *J. Phys. Chem. A* **2011**, *115*, 12034–12046.
- (65) Temelso, B.; Shields, G. C. The Role of Anharmonicity in Hydrogen-Bonded Systems: The Case of Water Clusters. *J. Chem. Theory Comput.* **2011**, *7*, 2804–2817.
- (66) Perez, C.; Muckle, M. T.; Zaleski, D. P.; Seifert, N. A.; Temelso, B.; Shields, G. C.; Kisiel, Z.; Pate, B. H. Structures of Cage, Prism, and Book Isomers of Water Hexamer from Broadband Rotational Spectroscopy. *Science* **2012**, *336*, 897–901.
- (67) Allodi, M. A.; Dunn, M. E.; Livada, J.; Kirschner, K. N.; Shields, G. C. Do Hydroxyl Radical-Water Clusters, $\text{OH}(\text{H}_2\text{O})_N$, $N = 1–5$, Exist in the Atmosphere? *J. Phys. Chem. A* **2006**, *110*, 13283–13289.
- (68) Alongi, K. S.; Dibble, T. S.; Shields, G. C.; Kirschner, K. N. Exploration of the Potential Energy Surfaces, Prediction of Atmospheric Concentrations, and Prediction of Vibrational Spectra for the $\text{HO}_2\cdots(\text{H}_2\text{O})_N$ ($N = 1–2$) Hydrogen Bonded Complexes. *J. Phys. Chem. A* **2006**, *110*, 3686–3691.
- (69) Kirschner, K. N.; Hartt, G. M.; Evans, T. M.; Shields, G. C. In Search of $\text{CS}_2(\text{H}_2\text{O})_{N=1–4}$ Clusters. *J. Chem. Phys.* **2007**, *126*, 154320.
- (70) Allodi, M. A.; Kirschner, K. N.; Shields, G. C. Thermodynamics of the Hydroxyl Radical Addition to Isoprene. *J. Phys. Chem. A* **2008**, *112*, 7064–7071.
- (71) Dunn, M. E.; Shields, G. C.; Takahashi, K.; Skodje, R. T.; Vaida, V. Experimental and Theoretical Study of the OH Vibrational Spectra and Overtone Chemistry of Gas-Phase Vinylacetic Acid. *J. Phys. Chem. A* **2008**, *112*, 10226–10235.
- (72) Hartt, G. M.; Shields, G. C.; Kirschner, K. N. Hydration of Ocs with One to Four Water Molecules in Atmospheric and Laboratory Conditions. *J. Phys. Chem. A* **2008**, *112*, 4490–4495.
- (73) Liu, Y. R.; Wen, H.; Huang, T.; Lin, X. X.; Gai, Y. B.; Hu, C. J.; Zhang, W. J.; Huang, W. Structural Exploration of Water, Nitrate/Water, and Oxalate/Water Clusters with Basin-Hopping Method Using a Compressed Sampling Technique. *J. Phys. Chem. A* **2014**, *118*, 508–516.
- (74) Xu, Y. S.; Nadykto, A. B.; Yu, F. Q.; Herb, J.; Wang, W. Interaction between Common Organic Acids and Trace Nucleation Species in the Earth's Atmosphere. *J. Phys. Chem. A* **2010**, *114*, 387–396.
- (75) Herb, J.; Nadykto, A. B.; Yu, F. Q. Large Ternary Hydrogen-Bonded Pre-Nucleation Clusters in the Earth's Atmosphere. *Chem. Phys. Lett.* **2011**, *518*, 7–14.
- (76) Jones, R. E.; Templeton, D. H. The Crystal Structure of Acetic Acid. *Acta Crystallogr.* **1958**, *11*, 484–487.
- (77) Vaida, V. Perspective: Water Cluster Mediated Atmospheric Chemistry. *J. Chem. Phys.* **2011**, *135*, 020901.
- (78) Robertson, W. H.; Johnson, M. A. Caught in the Act of Dissolution. *Science* **2002**, *298*, 69–69.
- (79) Gutberlet, A.; Schwaab, G.; Birer, O.; Masia, M.; Kaczmarek, A.; Forbert, H.; Havenith, M.; Marx, D. Aggregation-Induced Dissociation of $\text{HCl}(\text{H}_2\text{O})_4$ Below 1 K: The Smallest Droplet of Acid. *Science* **2009**, *324*, 1545–1548.
- (80) Forbert, H.; Masia, M.; Kaczmarek-Kedziera, A.; Nair, N. N.; Marx, D. Aggregation-Induced Chemical Reactions: Acid Dissociation in Growing Water Clusters. *J. Am. Chem. Soc.* **2011**, *133*, 4062–4072.